

# CHAPTER 1

## INTRODUCTION OF AVLBS

### 1. Introduction

The Armoured Vehicle Launched Bridge (AVLB) is a folding bridge that was fielded in the early 1970's as the Army's standard heavy assault bridge. The bridge is rated for normal crossings of military load class of 60 tons over a maximum gap of 60 feet and a vehicle speed of 25 mph. Army had a number of folding type AVLBS on turret less tank M47/48. Due to prolonged usage and non-availability of spare-parts of the carrier tanks, difficulty is being faced in maintenance. Problem was forwarded by the user units to resolve the issue for future maintenance of AVLBS.

The problem was referred to Military Vehicle Research and Development Establishment (MVRDE) who proposed that the existing AVLB system can be shifted / mounted on the current hull of one of the Main Battle Tanks (MBT) of Pakistan Army.

MVRDE undertook feasibility study of project of shifting/ mounting folding type AVLB on hull of MBT in year 2009/10 and successfully completed the prototype production in collaboration with its associate workshops and vendors.

New systems are costly and require a lot of foreign exchange. By considering the financial condition of our country, it is not difficult to decide that we have very limited options of procurement of defense equipment from other countries of the world. At the same time we can't be ignorant of the fact of any adventurous move of our neighbor to forestall our freedom. So all possible avenues of acquiring the equipment have to be explored and solutions of such problems have to be found immediately due to perceived threats.

In the light of feasibility study and availability of limited infrastructure MVRDE evaluated to opt for installation of held bridge system on the hull of MBT of Pak Army. The project is cost effective as compared to purchasing new system, from abroad. Detail of cost difference of new and modified options is given figure 1.



**Figure - 1.1** Differences of prices between bridges

### 1.1 BRIDGING EQUIPMENT USED BY ARMIES IN THE WORLD

Currently different types of bridging equipment are used by different armies of the world. Although they differ in capacity and size, different lengths of bridges, different cruising ranges and mobility of armour vehicles with different operating speed but they have one main purpose i.e. to lay the bridge for providing the crossing point to armour vehicles. Some of Armour Bridge Launched Vehicles of different countries in the world are as under :-

#### **Russia**

MTU20

AMX30

T72 AVLB

#### **Germany**

Leguan 26 MABLB

KMW Leopard 1 AVLBC (Biber)

**USA**

M60 AI AVLB

M104 Wolverine

**UK**

Titan Armour Bridge Layer

**India**

MTU -20

LT-55 AVLB

Kartik AVLB

BLG-60 AVLB

MHAB System

ESAB System

**Pakistan**

AM 50 Bridge

Ribbon Bridge

Hollow Plate Bridge

AVLB M47



AVLB M47



M60 AI AVLB

Figure - 1.2 AVLB in Action

## 1.2 COMPARISON OF UNDER CARRIAGES

Comparison of under carriages of some AVLBs of different countries is given in table 1.

**TABLE-1.1**

**PERFORMANCE CHARACTERISTICS OF UNDER CARRIAGES (TANKS)  
USED FOR CARRYING BRIDGES**

	<b>Engine Power (HP)</b>	<b>Range (Km)</b>	<b>Speed (Km/Hr)</b>	<b>Weight (Ton)</b>
<b>MBT Pakistan</b>	<b>1200</b>	<b>430</b>	<b>70</b>	<b>48</b>
<b>T-54 (Russia-MTU-20)</b>	<b>520</b>	<b>400</b>	<b>48</b>	<b>36</b>
<b>T-55 (India-LT-55 AVLB)</b>	<b>675</b>	<b>390</b>	<b>35</b>	<b>40.5</b>
<b>T-72 (Russia/India-MTU-20/Kartik)</b>	<b>840</b>	<b>483</b>	<b>67</b>	<b>46</b>
<b>Challenger (UK)</b>	<b>1200</b>	<b>450</b>	<b>59</b>	<b>62.5</b>
<b>Leopard (Germany)</b>	<b>830</b>	<b>450</b>	<b>65</b>	<b>38.7</b>
<b>M60(US-AVLB)</b>	<b>750</b>	<b>450</b>	<b>49</b>	<b>52.617</b>

## 1.3 RESEARCH QUESTIONS/JUSTIFICATIONS

To buy a new system of Armour Vehicle Launched Bridge or to upgrade the existing ones was a main concern. Purchase from international market was a viable option but required huge amount of foreign exchange. The other option was to develop the carrier of AVLB locally for indigenization. It was a very big challenge but seemed feasible as the technological backup was available in the country for carrying out such kind of research work and then take it to completion phase.

Challenges associated with this work involved designing of the system by good designers in the field of engineering, and then evaluation of the project cost which could

have been extremely high in some cases, another issue was modification of the hull of MBT available in the country. Availability of engines with power take off shaft and associated lifting cylinders were also essential to carry out such high load carrying equipment.

In the technical evaluation of the design the most important task was to carryout design analysis of AVLB carrier new design. Although main technique of reverse engineering was an option, but major concern remained, “Would the mechanical structure be able to withstand the peak loading conditions”? Moreover, the bridge system was also subjected to moments which could have been generated to damage the equipment and their remedy in designing was a focal point. So existing resources were used where possible, to complete the project in time. There are also broad prospects of achieving the success in this field by completing different such projects by our own resources in future.

Design analysis can be carried out in a number of different processes e.g. carrying out the experimental work on each of the component and then assess the design parameters and manufacture the required assembly or sub assembly but this is a costly option as a number of items would be destroyed while carrying out this task. Another option is numerically solve the equations and estimate stresses on each component to establish the fact that these components would be fail safe at the desired operating conditions. But another technique mostly adopted by manufacturers today is to carry out the design analysis by the experts in the field of stress analysis who can very effectively use Engineering Application Soft wares like ANSYS and Proe. These software provide a number of techniques to solve complex equations and carryout the stress analysis by simulating the environment in which they operate.

In this research Proe and ANSYS have been used to carry out analysis and there comparative results have given manufacturer evaluating tool to economize the cost and saving of precious time.

# CHAPTER 2

## FEM AND FEM SOFTWARES

### 2. INTRODUCTION

The finite element method or FEM started to help the engineers to find out the solution of very complex elastic and structural problems faced by civil, mechanical and aeronautical engineers in designing the structures made of metals, combination of metals or non metals. The pioneers of this method undoubtedly were Alexander Hrenikoff 1941 and his associate Richard Courant 1942 [1]. They adopted different theories and approaches but had similar vital characteristic: that discretization of the mesh of a continual domain into a set of discrete sub-domains, normally known to be elements. In 1947, Oligiered Zienkiewicz [2] compiled the work on this subject which was named Finite Element Method. He was the first one to formulate FEM.

Hrennikoff's work discretizes utilized a lattice method analogy, whereas Courant's [3] approach divided the domain in finite triangular regions in order to solve the 2<sup>nd</sup> partial differential equations that come from the problem of the torsion in a cylinder. Courant gave an amazing idea which is being utilized even today in FEM.

The actual development of the FEM really started in 1950s for the airframe and structure analysis and it gained speed in the Stuttgart University because of the work of John Argyres [3]. Also at Berkeley the same work was being pursued by ray W Clough [4] in the 1960s for civil engineering problems. By the late 1950s, the main ideas stiffness matrix and element matrix matured as is being utilized today.

A software NAST RAN [5] was made for NASA which was based on FEM. So mathematical base of method was also provided which was in print in 1973 as An Analysis of The Finite Element Method, after that it generalized all twigs of applied mathematics for numerical modelling of physical representations.

## 2.1 APPLICATIONS

Applications of FEM are numerous. This concept has been aptly utilized, adopted and researched. For example visualization of how an aero plane deforms in an asymmetrical crash using finite element analysis. By using the FEM technique United States Defense Department [\*6] carried out stress analysis of the bridge they made for AVLB of M-60 Bridge system.

A lot of variety of specializations of the mechanical engineers problems (such as aeronautical, biomechanical, and automotive) does extensively utilize FEM during the design and development of many products/project. Many modern FEM packages like ANSYS/Proe do have many parts as thermal, electromagnetic, fluid, and structural environments. In a structure simulation, FEM can help greatly in producing stiffness and strength simulations and also in optimizing weight, materials, and costs.

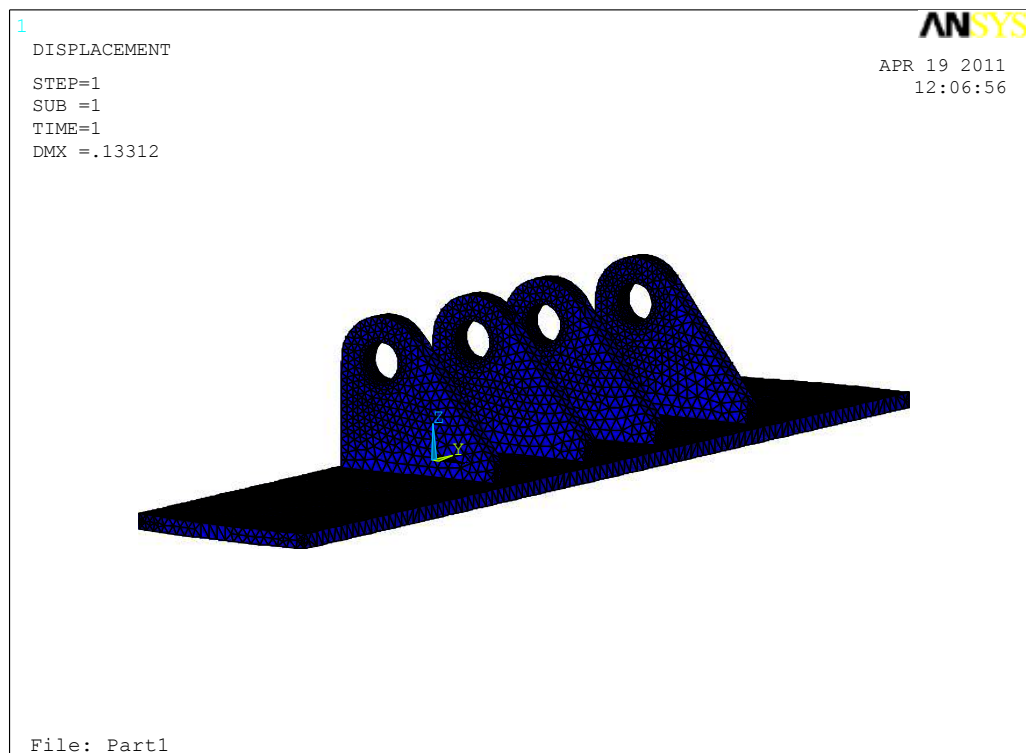


**Figure - 2.1** Application of FEM (ANSYS) in bracket analysis

FEM allows detailed visual outputs of where structures do bend /twist, and shows the distributions of stresses and also structural deformities. FEM soft wares like ANSYS and Mechanical provide a great range of simulation options and full control over the complexity of both modeling as well as analysis of scheme. Also, the desired level of accuracy and computational time required can also be managed to solve many types of engineering problems. FEM facilitates designers to modify their design, refine it, mature it by further analysis and finally optimize it so that it can be manufactured.

FEM has undergone improvement in technique of designing and raised standards of design. It has reduced the evaluation and inception times. Primarily a proto type is made quickly by using FEM and the development time has been reduced. Briefly speaking advantages FEM have enhanced accuracy, good designs and better insight of design parameters, prototyping in virtual (closer to actual) environment, lesser hardware changes in prototypes, a rapid and less expensive design cycle, increased productivity, and revenue. Same is the cause of using ANSYS/ Mechanical in the design analysis of AVLB.

## 2.2 STRESS

"Stress" is defined as the average force per unit area of a surface which is within a body on which inside forces act. These inside forces are produced due to reaction of body which act externally which are either surface forces or body forces. As the loaded twisted/bent body is a continuum, the inside forces are distributed within the volume of the material body, i.e. the stress distribution in the body is expressed as a piecewise persistent/continual function of space and the time. As an example when a body is axially loaded, for example a prismatic bar which is under to tension or compression by a force through the center of gravity the stress  $\sigma$ , or intensity of inside forces, can be obtained by dividing the total normal force  $F_n$  by the bar's cross-sectional area  $A$ . The normal force is the balance of forces. The normal force applied on bar can be a tensile force if it is acting outward or it can be compressive if acting inward to the plane. In the case of a prismatic bar axially loaded, the stress  $\sigma$  is denoted by a scalar called engineering stress or average stress ( $\sigma_{avg}$ ) over the area, meaning that the stress in the cross-section is uniformly distributed. Thus,



$$[6] \sigma_{\text{avg}} = \frac{F_n}{A} \approx \sigma$$

### 2.3 THEORETICAL BACKGROUND

The continuum mechanics has been studied in detail as in the design analysis of AVL, the model considered are deformable / flexible material bodies. The continuum mechanics always deals with deformable bodies not stiff bodies. The stresses in continuum mechanics are considered if those which are produced by deformation of the body, relative changes are considered not the absolute values. A body is considered stress-free if the present forces are only inter atomic forces (ionic, metallic etc) required in order to hold the body together and to keep the shape in the absence of all external influences, like gravitation and other forces. Stresses which are generated during manufacture of the body are also not included.

Newtonian and Eulerian [7] dynamic explain that motion of the material in the body is caused due to action of the externally applied forces which are called surface and body forces.

When a force is applied, it acts on the surface of the body due to mechanical contact, or these act on the visualized/imaginary surfaces which bind the parts of the body, as a result of the mechanical interaction between these parts. Due to application of external forces on the body the inside forces pass from one point to another point in the body to balance their reaction, as indicated by the Newton's second law of motion of conservation of momentum. These laws are called Euler's equations of motion.

These laws have been adopted by Euler equations [7] so stress is the calculation of level of distribution of force inside the body.

Thus stress is called average force exerted on unit area of exterior surface. The intensity of contact forces is in inverse proportion to the area of contact. If a force is applied on a small area it will cause more stress. If same force is applied on larger area stress will be lesser. So effect of force will be different on each surface.

Body forces start from sources outside of the body that act on its volume (or mass). This implies that the inside forces manifest through the contact forces alone. These forces arise from the presence of the body in force fields, (e.g. gravitational field). As the mass of the body is assumed to be uniformly, any force initiating from the mass is also persistently distributed. Thus, body forces are generally persistent over the body's volume.

The density of inside forces at all points in a deformable body is not even, *i.e.* there can be distribution of stresses. This variation of the inside forces comes under the laws of the conservation of linear and angular momentums, which usually apply to minute parts but do extend the body of evenly distributed mass.

## 2.4 PROBLEM EXPLANATION

Here is demonstration of the finite element method by using two examples from which the generalized method can be inferred. P1 is a 1D [2] problem and it states:-

$$P1 : \begin{cases} u''(x) = f(x) & \text{in } (0, 1), \\ u(0) = u(1) = 0, \end{cases}$$

where  $f$  is given,  $u$  is unknown function of  $x$ , and  $u''$  is second rate of change of  $u$  with respect to  $x$ .

Here is the two dimensional example of Dirichlet's problem [2].

$$P2 : \begin{cases} u_{xx}(x, y) + u_{yy}(x, y) = f(x, y) & \text{in } \Omega, \\ u = 0 & \text{on } \partial\Omega, \end{cases}$$

where  $\Omega$  is connected open region in the  $(x,y)$  plane whose boundary  $\partial\Omega$  is smooth, and  $u_{xx}$  and  $u_{yy}$  are the second rate of changes with respect to  $x$  and  $y$ .

The problem P1 can be solved "directly" by computing anti-rate of changes but this method works if there is one spatial dimension and has no generalized high dimensional problems like  $u + u'' = f$ . For this sole reason, the finite element method will be developed for P1 and generalize it for P2.

It can be explained it in 2 steps to solve boundary value problem (BVP) using the FEM.

- a. 1<sup>st</sup> Step - rephrase the original BVP in weak shape. There is no calculation needed for this step. The conversion can be done by hand on paper.
- b. 2<sup>nd</sup> Step is the discretization, where the weak shape has been discretized in a finite dimensional space.

Once the 2<sup>nd</sup> step has been completed, a concrete formula is obtained for a finite dimensional problem. The formula can approximately solve the linearized problem.

## 2.4 WEAK FORMULATIONS

First of all convert P1 to P2 and make weak formulation. If  $u$  solves P1, then for any smooth function  $v$  that satisfies the boundary conditions, that is  $v = 0$  at  $x = 0$  and  $x = 1$ , then it becomes.

$$\int_0^1 f(x)v(x) dx = \int_0^1 u''(x)v(x) dx.$$

Similarly, if  $u$  with  $u(0) = u(1) = 0$  satisfies mathematical relationship 1 for every smooth function  $v(x)$  then one can prove that  $u$  will solve P1. The proof is easy for the dual continual differential  $u$ , but may be solved in an evenly sense also.

By using the integration on the right-hand-side of mathematical relationship (1), following is obtained:-

$$\begin{aligned} \int_0^1 f(x)v(x) dx &= \int_0^1 u''(x)v(x) dx \\ &= u'(x)v(x)|_0^1 - \int_0^1 u'(x)v'(x) dx \\ &= - \int_0^1 u'(x)v'(x) dx = -\phi(u, v). \end{aligned}$$

here assume as :  $v(0) = v(1) = 0$ .

## 2.5 A PROOF UNIQUENESS OF THE SOLUTION

Now loosely take of  $H_0^1(0, 1)$  as absolutely continuous functions of  $(0,1)$  that are 0 at  $x = 0$  and  $x = 1$ . Such function while differenced turns out the symmetric bi-linear map  $\phi$  then defines an inner product which turns  $H_0^1(0, 1)$  into Hilbert space. At the same

time  $\int_0^1 f(x)v(x)dx$  is an inner product, this time on the lp sapce [\*7] as  $L^2(0,1)$ . One solution of Hilbert [7] space shows that there is unique  $u$  solving and therefore, P1. This solution is a-priori if a member of  $H_0^1(0,1)$ , but using elliptic regularity, will be smooth if  $f$  is smooth.

## 2.6 THE WEAK FORM OF P2

When integrated is solved as following [\*7]:-

$$\int_{\Omega} f v ds = - \int_{\Omega} \nabla u \cdot \nabla v ds = -\phi(u, v),$$

where  $\nabla$  is the gradient and is dot product in the 2D plane. Also  $\phi$  is inner product on space  $H_0^1(\Omega)$  of differenced functions of  $\Omega$  that are zero on  $\partial\Omega$ .

# CHAPTER 3

## LITERATURE REVIEW

### 3. VARIOUS TYPES OF FEM METHODS

FEM has different types, some of them are discussed below:-

#### 3.1.1 GENERALIZED FEM

This Finite Element Method (GFEM) [\*7] utilizes local spaces which comprises of functions, not only polynomials, that show the available information on the unknown solution and ensures good local approximation. Therefore a partition of this unity is utilized to “bond” these spaces together in an approximating sub-space. The effectiveness of this method has been shown while applied to problems with domains have complicated boundary, problems with micro-scales, and problem with the boundary layer.

#### 3.1.2 hp-FEM

In this type,  $h$  version of polynomial approximation will be constant for all elements and the number of elements is increased.  $p$  version are constant to increase the polynomial approximation of all elements.

#### 3.1.3 hpk-FEM

It has variable element size  $h$ , polynomial degree of local approximation  $p$  and the global differentiability of the local approximations  $(k-1)$  to achieve excellent convergence rates.

#### 3.1.4 XFEM

These methods include following:-

- a. Spectral method
- b. Mesh-free method
- c. Galerkin's methods
- d. FEM Limit [17] Analysis

### 3.2 EXPLANATION OF DEFORMATION

Deformation means change of shape, size or dimensions which means that a curve drawn at the start of body placement changes its length and displaced final placement. If all the curves don't change length, it is a stiff body disposition.

The component  $X_i$  of the position vector  $\mathbf{X}$  of a minute part in the reference construction, taken with respect to the reference coordinate system, are called the material or reference coordinates. Moreover, the components  $x_i$  of the position vector  $\mathbf{x}$  of a minute part in the twisted/bent construction, taken with respect to the spatial coordinate system of reference, are called the spatial coordinates.

To generalize the analyzing methods, there are two approaches for analyzing the bend/twist of a continuum. One can be explained as change in material or referential coordinates, called material or Lagrangian [8]. It can also be explained in terms of the spatial coordinates it is called the spatial explanation or Eulerian [7] description.

There is continuity during bend/twist of a continuum body that :

- a. The material points forming a closed curve at any instant will always shape a closed curve at any subsequent moment.
- b. The material points forming a closed will shape a closed surface at any subsequent time and the matter within the surface will remain within.

### 3.3 AFFINE BEND/TWIST

When a bend or twist is described by an affine conversion it is called an affine bend/twist. This conversion will be linear conversion and a stiff body translation. These bends/twists are also known as homogeneous bends/twists. It has following expression:-

$$\mathbf{x}(\mathbf{X}, t) = \mathbf{F}(t) \cdot \mathbf{X} + \mathbf{c}(t) \quad [9]$$

Here,  $\mathbf{x}$  is the position of twisted/bent construction,  $\mathbf{X}$  is the position in a reference construction,  $t$  is a time parameter,  $\mathbf{F}$  is the linear-transformer and  $\mathbf{c}$  is disposition. In matrix form, where the components are with respect to an ortho-perpendicular basis,

$$\begin{matrix} [9], \\ \begin{bmatrix} x_1(X_1, X_2, X_3, t) \\ x_2(X_1, X_2, X_3, t) \\ x_3(X_1, X_2, X_3, t) \end{bmatrix} = \begin{bmatrix} F_{11}(t) & F_{12}(t) & F_{13}(t) \\ F_{21}(t) & F_{22}(t) & F_{23}(t) \\ F_{31}(t) & F_{32}(t) & F_{33}(t) \end{bmatrix} \begin{bmatrix} X_1 \\ X_2 \\ X_3 \end{bmatrix} + \begin{bmatrix} c_1(t) \\ c_2(t) \\ c_3(t) \end{bmatrix} \\ [9] \end{matrix}$$

The above bend/twist becomes *non-affine* or *inhomogeneous* if  $\mathbf{F} = \mathbf{F}(\mathbf{X}, t)$  or  $\mathbf{c} = \mathbf{c}(\mathbf{X}, t)$ .

### 3.4 STIFF BODY MOTION

It is a special type of affine bend/twist that does not involve any shear, extension or compression. The conversion matrix  $\mathbf{F}$  is orthogonal to allow rotations. Stiff body motion can be expressed as:-

$$\mathbf{x}(\mathbf{X}, t) = \mathbf{Q}(t) \cdot \mathbf{X} + \mathbf{c}(t) \quad [10]$$

where

$$\mathbf{Q} \cdot \mathbf{Q}^T = \mathbf{Q}^T \cdot \mathbf{Q} = \mathbf{1}$$

In matrix form,

$$\begin{matrix} \begin{bmatrix} x_1(X_1, X_2, X_3, t) \\ x_2(X_1, X_2, X_3, t) \\ x_3(X_1, X_2, X_3, t) \end{bmatrix} = \begin{bmatrix} Q_{11}(t) & Q_{12}(t) & Q_{13}(t) \\ Q_{21}(t) & Q_{22}(t) & Q_{23}(t) \\ Q_{31}(t) & Q_{32}(t) & Q_{33}(t) \end{bmatrix} \begin{bmatrix} X_1 \\ X_2 \\ X_3 \end{bmatrix} + \begin{bmatrix} c_1(t) \\ c_2(t) \\ c_3(t) \end{bmatrix} \\ [10] \end{matrix}$$

Displacements of deformed body are shown in figure-3.1 [\*7]

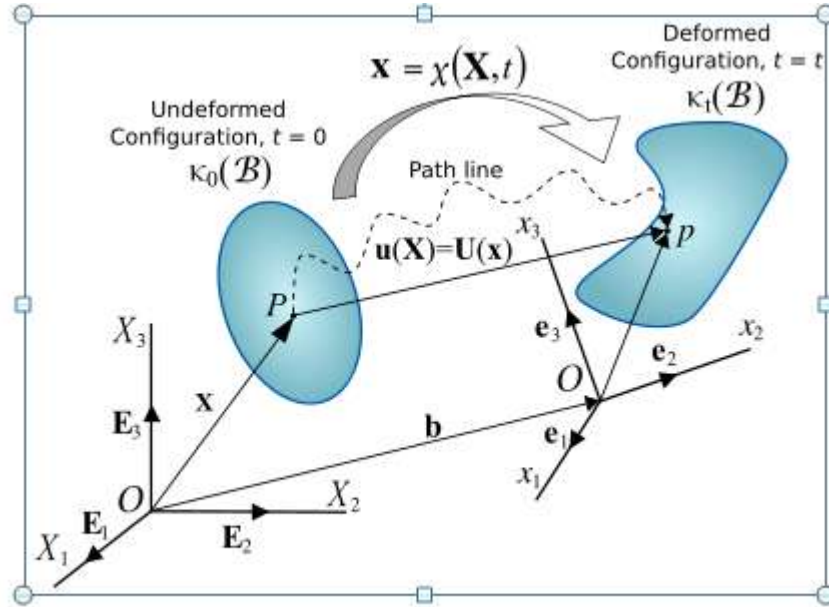


**Figure – 3.1 Unreformed shape compared with deformed shape**

### 3.5 MOTION OF A CONTINUUM BODY

A change in the construction of a continuum body gives rise to disposition, it has 2 components: a stiff-body disposition and a bend/twist. The stiff-body disposition as a simultaneous linear movements and rotation of the body without changing its shape/size. Bend/twist implies that change in shape and/or size of the body from initial or unreformed construction  $\kappa_0(\mathcal{B})$  to deformed construction  $\kappa_t(\mathcal{B})$  [11].

If after a disposition of the continuum there is a relative disposition between minute parts, a bend/twist has occurred. On the other hand, if after movement of the continuum the relative movement between minute parts in the current construction is zero, then there is no bend/twist and a stiff-body movement is said to have occurred.

The vector joining the positions of a minute part P in the un-deformed construction and twisted/bent construction is called the vector  $\mathbf{u}(\mathbf{X}, t) = u_i \mathbf{e}_i$  in the Lagrangian [8] description, or  $\mathbf{U}(\mathbf{x}, t) = U_j \mathbf{E}_j$  in the Eulerian [5] description.



A movement field is a vector field of all displacement vectors for all minute parts in the body, which relates the twisted/bent construction with the un-deformed construction. It is convenient to do the analysis of bend/twist or motion of a continuum body in terms of the displacement field, It can be written as:-

or in terms of the spatial coordinates will give it the form:-

$$\mathbf{U}(\mathbf{x}, t) = \mathbf{b}(\mathbf{x}, t) + \mathbf{x} - \mathbf{X}(\mathbf{x}, t) \quad \text{or} \quad U_J = b_J + \alpha_{Ji}x_i - X_J$$

[11]

where  $\alpha_{ji}$  are the direction cosines between the material and space coordinate schemes with unit vectors  $\mathbf{E}_J$  and  $\mathbf{e}_i$ , respectively. Thus

$$\mathbf{E}_J \cdot \mathbf{e}_i = \alpha_{Ji} = \alpha_{iJ}$$

and the relationship between  $u_i$  and  $U_J$  is:-

$$u_i = \alpha_{iJ}U_J \quad \text{or} \quad U_J = \alpha_{Ji}u_i$$

Knowing that

$$\mathbf{e}_i = \alpha_{iJ}\mathbf{E}_J$$

then

$$\mathbf{u}(\mathbf{X}, t) = u_i\mathbf{e}_i = u_i(\alpha_{iJ}\mathbf{E}_J) = U_J\mathbf{E}_J = \mathbf{U}(\mathbf{x}, t)$$

While superimposing the coordinate systems results in  $\mathbf{b} = 0$ , and the direction cosines become:

$$\mathbf{E}_J \cdot \mathbf{e}_i = \delta_{Ji} = \delta_{iJ}.$$

Thus, it becomes

$$\mathbf{u}(\mathbf{X}, t) = \mathbf{x}(\mathbf{X}, t) - \mathbf{X} \quad \text{or} \quad u_i = x_i - \delta_{iJ}X_J = x_i - X_i$$

or in terms of the spatial coordinates to be

$$\mathbf{U}(\mathbf{x}, t) = \mathbf{x} - \mathbf{X}(\mathbf{x}, t) \quad \text{or} \quad U_J = \delta_{Ji}x_i - X_J = x_J - X_J$$

### 3.6 DISPLACEMENT GRADIENT TENSOR

The displacement vector when subjected to partial differentiation with respect to the material coordinates explains the material displacement gradient tensor  $\nabla_{\mathbf{X}}\mathbf{u}$ . Thus:

$$\begin{aligned} \mathbf{u}(\mathbf{X}, t) &= \mathbf{x}(\mathbf{X}, t) - \mathbf{X} & u_i &= x_i - \delta_{iJ}X_J = x_i - X_i \\ \nabla_{\mathbf{X}}\mathbf{u} &= \nabla_{\mathbf{X}}\mathbf{x} - \mathbf{I} & \text{or} & \frac{\partial u_i}{\partial X_K} = \frac{\partial x_i}{\partial X_K} - \delta_{iK} \\ \nabla_{\mathbf{X}}\mathbf{u} &= \mathbf{F} - \mathbf{I} & & \end{aligned} \quad [12]$$

Here,  $\mathbf{F}$  is called the bend/twist gradient tensor.

In the same way, the partial differentiation of the displacements vector with respect to the space coordinates gives the spatial displacement gradient tensor  $\nabla_{\mathbf{x}}\mathbf{U}$ . That is:

$$\begin{aligned} \mathbf{U}(\mathbf{x}, t) &= \mathbf{x} - \mathbf{X}(\mathbf{x}, t) & U_J &= \delta_{Ji}x_i - X_J = x_J - X_J \\ \nabla_{\mathbf{x}}\mathbf{U} &= \mathbf{I} - \nabla_{\mathbf{x}}\mathbf{X} & \text{or} & \frac{\partial U_J}{\partial x_k} = \delta_{Jk} - \frac{\partial X_J}{\partial x_k} \\ \nabla_{\mathbf{x}}\mathbf{U} &= \mathbf{I} - \mathbf{F}^{-1} & & \end{aligned}$$

### 3.7 PLANE BEND/TWIST

A plane bend/twist is also known as plane strain; here it should be known that bend/twist is restricted to one of planes in the reference construction. If the bend/twist is restricted to the plane described by the basis vectors  $\mathbf{e}_1, \mathbf{e}_2$ , the bend/twist gradient has the form:-

$$\mathbf{F} = F_{11}\mathbf{e}_1 \otimes \mathbf{e}_1 + F_{12}\mathbf{e}_1 \otimes \mathbf{e}_2 + F_{21}\mathbf{e}_2 \otimes \mathbf{e}_1 + F_{22}\mathbf{e}_2 \otimes \mathbf{e}_2 + \mathbf{e}_3 \otimes \mathbf{e}_3$$

In matrix form it will be written as,

$$\mathbf{F} = \begin{bmatrix} F_{11} & F_{12} & 0 \\ F_{21} & F_{22} & 0 \\ 0 & 0 & 1 \end{bmatrix}_{[13]}$$

From the polar resolution the bend/twist gradient, up to a change of coordinates, can be resolved into stretch and rotation. Since all the bend/twist is in a plane, it can be written as below,

$$\mathbf{F} = \mathbf{R} \cdot \mathbf{U} = \begin{bmatrix} \cos \theta & \sin \theta & 0 \\ -\sin \theta & \cos \theta & 0 \\ 0 & 0 & 1 \end{bmatrix} \begin{bmatrix} \lambda_1 & 0 & 0 \\ 0 & \lambda_2 & 0 \\ 0 & 0 & 1 \end{bmatrix}_{[13]}$$

Where,  $\theta$  is the angle of rotation and  $\lambda_1, \lambda_2$  are the main stretches.

### 3.8 ISOCHORIC PLANE BEND/TWIST

For the conditions that bend/twist is isochoric (i.e. it conserves the volume) it can be written as  $\det(\mathbf{F}) = 1$  and having

$$F_{11}F_{22} - F_{12}F_{21} = 1$$

Alternatively,  $\lambda_1\lambda_2 = 1$

### 3.9 SIMPLE SHEAR

In simpler words shear bend/twist is defined as an isochoric plane bend/twist where a set of line elements with a given reference direction do not change length and direction while subjected to bending/twist.

If  $\mathbf{e}_1$  is the fixed reference direction in which line elements do not deform during the bend/twist then  $\lambda_1 = 1$  and

$$\mathbf{F} \cdot \mathbf{e}_1 = \mathbf{e}_1$$

Therefore,

$$F_{11}\mathbf{e}_1 + F_{21}\mathbf{e}_2 = \mathbf{e}_1 \quad \implies \quad F_{11} = 1 ; F_{21} = 0$$

Since the bend/twist is isochoric,

$$F_{11}F_{22} - F_{12}F_{21} = 1 \quad \implies \quad F_{22} = 1$$

Define  $\gamma := F_{12}$

For simple shear the bend gradient is expressed as:

$$\mathbf{F} = \begin{bmatrix} 1 & \gamma & 0 \\ 0 & 1 & 0 \\ 0 & 0 & 1 \end{bmatrix}_{[13]}$$

Now,

$$\mathbf{F} \cdot \mathbf{e}_2 = F_{12}\mathbf{e}_1 + F_{22}\mathbf{e}_2 = \gamma\mathbf{e}_1 + \mathbf{e}_2 \implies \mathbf{F} \cdot (\mathbf{e}_2 \otimes \mathbf{e}_2) = \gamma\mathbf{e}_1 \otimes \mathbf{e}_2 + \mathbf{e}_2 \otimes \mathbf{e}_2$$

Since  $\mathbf{e}_i \otimes \mathbf{e}_i = \mathbf{1}$

The bend/twist gradient can be written as,

$$\mathbf{F} = \mathbf{1} + \gamma\mathbf{e}_1 \otimes \mathbf{e}_2$$

### 3.10 EULER–CAUCHY STRESS PRINCIPLE

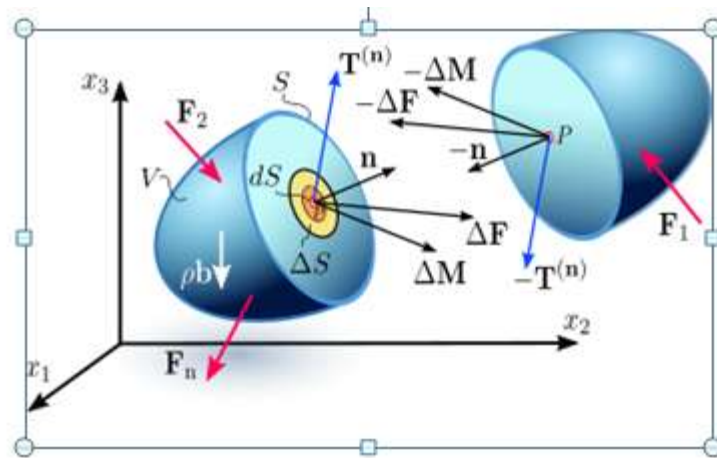


Figure - 3.2 Inside distribution of contact forces stresses

Figure 3.2[\*7] shows the inside distribution of contact forces and couple stresses on a differential  $dS$  of the inside surface  $S$  in a continuum,

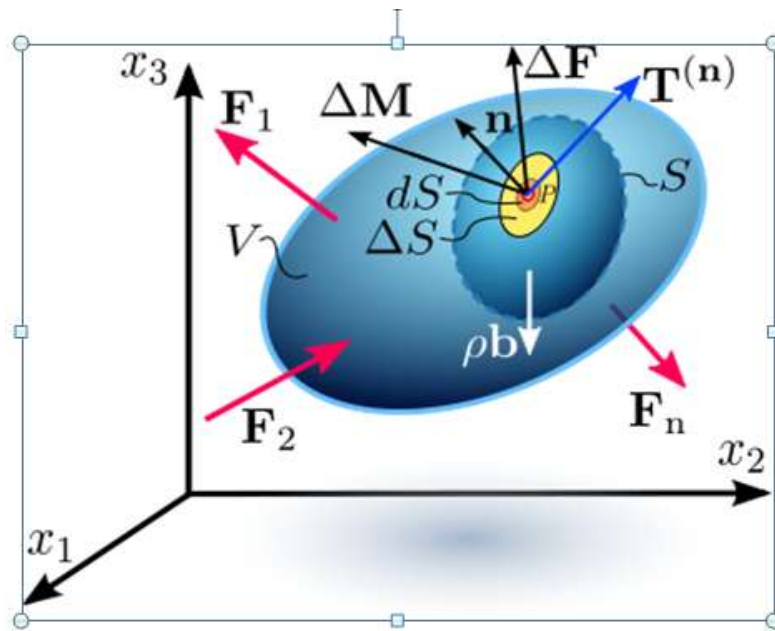


Figure – 3.3 Inside distribution of force/stresses

Figure 3.3 [18] shows the inside distribution of contact forces and couple stresses on a differential  $dS$  of the inside surface  $S$  in a continuum.

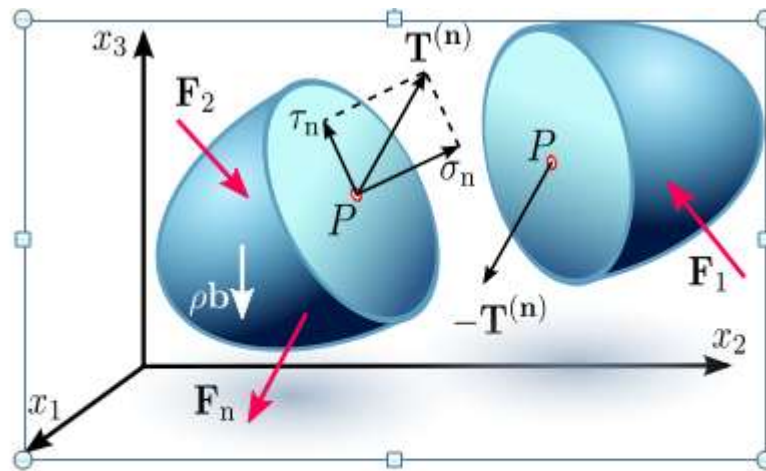


Figure – 3.4 Stress vector on surface

Figure 3.4 shows the stress vector on an inside surface  $S$  with perpendicular vector  $n$ . Depending on the direction of the plane under consideration, the stress vector may not be perpendicular to that plane, i.e. parallel to it and can be resolved into two components: one component perpendicular to the plane, called perpendicular stress  $\sigma_n$ , and another component parallel to this plane, called the shearing stress  $\tau$ .

The Euler–Cauchy [6] stress principle states that upon any exterior surface (real or imaginary) that divides the body, the action of one part of the body on the other is equivalent to the scheme of distributed forces and couples on the exterior surface dividing the body, and it is denoted by a vector field  $\mathbf{T}^{(\mathbf{n})}$ , called the stress vector, defined on the exterior surface  $S$  and assumed to depend continually on the exterior surface's unit vector  $\mathbf{n}$ .

This principle can be explained by considering an imaginary exterior surface  $S$  which passes through point  $P$  located inside the material dividing the continual body into two segments, as seen in figure 3.4. The body is subjected to external surface forces  $\mathbf{F}$  and body forces  $\mathbf{b}$ . The inside contact forces transmitted from one segment to the other through the dividing plane, due to the action of one portion of the continuum onto the other, generate a force distribution on a small area  $\Delta S$ , with a perpendicular unit vector  $\mathbf{n}$ , on the dividing plane  $S$ .

The force distribution is equal to a contact force  $\Delta\mathbf{F}$  and a couple stress  $\Delta\mathbf{M}$ , as shown in figure 3.4. Cauchy's stress principle asserts that  $\Delta S$  becomes very small and tends to zero the ratio  $\Delta\mathbf{F}/\Delta S$  becomes  $d\mathbf{F}/dS$  and the couple stress vector  $\Delta\mathbf{M}$  vanishes. In specific fields of continuum mechanics [9] the couple stress is assumed not to vanish. The resultant vector  $d\mathbf{F}/dS$  is defined to be the stress vector or traction vector given by  $\mathbf{T}^{(\mathbf{n})} = T_i^{(\mathbf{n})} \mathbf{e}_i$  at the point  $P$  associated with a plane with a perpendicular vector  $\mathbf{n}$ :

$$T_i^{(\mathbf{n})} = \lim_{\Delta S \rightarrow 0} \frac{\Delta F_i}{\Delta S} = \frac{dF_i}{dS} \quad [14]$$

This mathematical relationship explains that the stress vector is dependent on its position in the body and the direction of the plane where it is acting.

Depending on the direction of the plane under consideration, the stress vector may not necessarily be perpendicular to that plane, i.e. parallel to  $\mathbf{n}$ , and can be resolved into two components:

- a. Perpendicular to the plane, called perpendicular stress

$$\sigma_n = \lim_{\Delta S \rightarrow 0} \frac{\Delta F_n}{\Delta S} = \frac{dF_n}{dS},$$

where  $dF_n$  is the perpendicular component of the force  $d\mathbf{F}$  to the differential area  $dS$

- b. The other parallel to this plane, called the shear stress

$$\tau = \lim_{\Delta S \rightarrow 0} \frac{\Delta F_s}{\Delta S} = \frac{dF_s}{dS},$$

where  $dF_s$  is the tangential component of the force  $d\mathbf{F}$  to the differential surface area  $dS$ . The shear stress can be further resolved into two mutually perpendicular vectors.

### 3.11 SIGN CONVENTION

Consider a tetrahedron with three faces oriented in the coordinate planes, and with an infinite facsimile area  $dA$  oriented in an arbitrary direction specified by a normal unit vector  $\mathbf{n}$  (Figure 3.5). The tetrahedron is shaped by slicing a parallelepiped along an arbitrary plane  $\mathbf{n}$ . So, the force acting on the plane  $\mathbf{n}$  it will be subjected to (-) reaction force, where the right-hand-side denotes the product of the mass enclosed by the tetrahedron which is and its acceleration:  $\rho$  is the density,  $\mathbf{a}$  is the acceleration, and  $h$  is the height of the tetrahedron, considering the plane  $\mathbf{n}$  to be the base. The area of the faces of the tetrahedron perpendicular to the axes is given by projecting  $dA$  into each face (using the dot product):

$$dA_1 = (\mathbf{n} \cdot \mathbf{e}_1) dA = n_1 dA, [14]$$

$$dA_2 = (\mathbf{n} \cdot \mathbf{e}_2) dA = n_2 dA,$$

$$dA_3 = (\mathbf{n} \cdot \mathbf{e}_3) dA = n_3 dA,$$

simplify to cancel out  $dA$ :

$$\mathbf{T}^{(\mathbf{n})} - \mathbf{T}^{(\mathbf{e}_1)} n_1 - \mathbf{T}^{(\mathbf{e}_2)} n_2 - \mathbf{T}^{(\mathbf{e}_3)} n_3 = \rho \left( \frac{h}{3} \right) \mathbf{a}.$$

To consider the limiting case to be the tetrahedron shrinks to a point,  $h$  must go to 0 (intuitively, the plane  $\mathbf{n}$  is translated along  $\mathbf{n}$  toward O). As a result,

$$\mathbf{T}^{(\mathbf{n})} = \mathbf{T}^{(\mathbf{e}_1)}n_1 + \mathbf{T}^{(\mathbf{e}_2)}n_2 + \mathbf{T}^{(\mathbf{e}_3)}n_3. \quad (\text{due to } h=0)$$

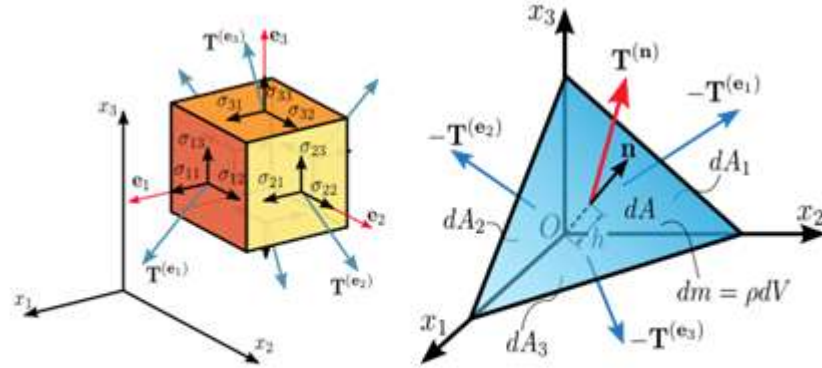


Figure – 3.5 Stresses in 3D

Figure 3.5 [\*7] shows components of stress in three dimensions

Assuming a material element with planes perpendicular to the coordinate axes of a Cartesian coordinate, the stress vectors associated with each of the element planes, i.e.  $\mathbf{T}^{(\mathbf{e}_1)}$ ,  $\mathbf{T}^{(\mathbf{e}_2)}$ , and  $\mathbf{T}^{(\mathbf{e}_3)}$  can be resolved into a perpendicular component and two shear components, i.e. components in the direction of the three coordinate axes. For the particular case of a exterior surface with perpendicular unit vector directed in the direction of the  $x_1$ -axis, show the perpendicular stress by  $\sigma_{11}$ , and the two shear stresses as  $\sigma_{12}$  and  $\sigma_{13}$ :

$$\mathbf{T}^{(\mathbf{e}_1)} = T_1^{(\mathbf{e}_1)}\mathbf{e}_1 + T_2^{(\mathbf{e}_1)}\mathbf{e}_2 + T_3^{(\mathbf{e}_1)}\mathbf{e}_3 = \sigma_{11}\mathbf{e}_1 + \sigma_{12}\mathbf{e}_2 + \sigma_{13}\mathbf{e}_3, [15]$$

$$\mathbf{T}^{(\mathbf{e}_2)} = T_1^{(\mathbf{e}_2)}\mathbf{e}_1 + T_2^{(\mathbf{e}_2)}\mathbf{e}_2 + T_3^{(\mathbf{e}_2)}\mathbf{e}_3 = \sigma_{21}\mathbf{e}_1 + \sigma_{22}\mathbf{e}_2 + \sigma_{23}\mathbf{e}_3,$$

$$\mathbf{T}^{(\mathbf{e}_3)} = T_1^{(\mathbf{e}_3)}\mathbf{e}_1 + T_2^{(\mathbf{e}_3)}\mathbf{e}_2 + T_3^{(\mathbf{e}_3)}\mathbf{e}_3 = \sigma_{31}\mathbf{e}_1 + \sigma_{32}\mathbf{e}_2 + \sigma_{33}\mathbf{e}_3,$$

In index notation this is

$$\mathbf{T}^{(\mathbf{e}_i)} = T_j^{(\mathbf{e}_i)}\mathbf{e}_j = \sigma_{ij}\mathbf{e}_j.$$

The nine components  $\sigma_{ij}$  of the stress vectors are called the Cauchy stress tensor.



$$\boldsymbol{\sigma} = \sigma_{ij} = \begin{bmatrix} \mathbf{T}^{(\mathbf{e}_1)} \\ \mathbf{T}^{(\mathbf{e}_2)} \\ \mathbf{T}^{(\mathbf{e}_3)} \end{bmatrix} = \begin{bmatrix} \sigma_{11} & \sigma_{12} & \sigma_{13} \\ \sigma_{21} & \sigma_{22} & \sigma_{23} \\ \sigma_{31} & \sigma_{32} & \sigma_{33} \end{bmatrix} \equiv \begin{bmatrix} \sigma_{xx} & \sigma_{xy} & \sigma_{xz} \\ \sigma_{yx} & \sigma_{yy} & \sigma_{yz} \\ \sigma_{zx} & \sigma_{zy} & \sigma_{zz} \end{bmatrix} \equiv \begin{bmatrix} \sigma_x & \tau_{xy} & \tau_{xz} \\ \tau_{yx} & \sigma_y & \tau_{yz} \\ \tau_{zx} & \tau_{zy} & \sigma_z \end{bmatrix},$$

Where  $\sigma_{11}$ ,  $\sigma_{22}$ , and  $\sigma_{33}$  are perpendicular stresses, and  $\sigma_{12}$ ,  $\sigma_{13}$ ,  $\sigma_{21}$ ,  $\sigma_{23}$ ,  $\sigma_{31}$ , and  $\sigma_{32}$  are shear stresses. The first index  $i$  shows that the stress acts on a plane perpendicular to the  $x_i$ -axis, and the second index  $j$  shows the direction in which the stress acts. A stress is positive if it acts in the positive direction of the coordinate axes, and if the plane where it acts has an outward perpendicular vector pointing in the positive coordinate direction.

Thus, using the resolved vectors of the stress tensor [15]

$$\begin{aligned} \mathbf{T}^{(\mathbf{n})} &= \mathbf{T}^{(\mathbf{e}_1)}n_1 + \mathbf{T}^{(\mathbf{e}_2)}n_2 + \mathbf{T}^{(\mathbf{e}_3)}n_3 \\ &= \sum_{i=1}^3 \mathbf{T}^{(\mathbf{e}_i)}n_i \\ &= (\sigma_{ij}\mathbf{e}_j)n_i \\ &= \sigma_{ij}n_i\mathbf{e}_j \end{aligned}$$

or, equivalently,

$$T_j^{(\mathbf{n})} = \sigma_{ij}n_i.$$

Alternatively, in matrix shape we have

$$\begin{bmatrix} T_1^{(\mathbf{n})} & T_2^{(\mathbf{n})} & T_3^{(\mathbf{n})} \end{bmatrix} = \begin{bmatrix} n_1 & n_2 & n_3 \end{bmatrix} \cdot \begin{bmatrix} \sigma_{11} & \sigma_{12} & \sigma_{13} \\ \sigma_{21} & \sigma_{22} & \sigma_{23} \\ \sigma_{31} & \sigma_{32} & \sigma_{33} \end{bmatrix}.$$

The Voigt notation representation of the Cauchy stress tensor takes advantage of the equilibrium of the stress tensor to express the stress to be a six-dimensional vector of the shape:

$$\boldsymbol{\sigma} = [\sigma_1 \quad \sigma_2 \quad \sigma_3 \quad \sigma_4 \quad \sigma_5 \quad \sigma_6]^T \equiv [\sigma_{11} \quad \sigma_{22} \quad \sigma_{33} \quad \sigma_{23} \quad \sigma_{31} \quad \sigma_{12}]^T.$$

The Voigt notation is utilized extensively in denoting stress-strain relations in solid mechanics and for computational efficiency in numerical structural mechanics software.

### 3.12 CONVERSION RULE OF THE STRESS TENSOR

It can be shown that the stress tensor is a contra variant second order tensor, which is a statement of how it alters under a change of the coordinate system. From an  $x_i$ -system to an  $x'_i$ -system, the components  $\sigma_{ij}$  in the initial scheme are altered into the components  $\sigma'_{ij}$  in the new scheme according to the tensor conversion rule in Figure 3.6.

$$\sigma'_{ij} = a_{im}a_{jn}\sigma_{mn} \quad \text{or} \quad \boldsymbol{\sigma}' = \mathbf{A}\boldsymbol{\sigma}\mathbf{A}^T,$$

where  $\mathbf{A}$  is a rotation matrix with components  $a_{ij}$ . In matrix shape this is

$$\begin{bmatrix} \sigma'_{11} & \sigma'_{12} & \sigma'_{13} \\ \sigma'_{21} & \sigma'_{22} & \sigma'_{23} \\ \sigma'_{31} & \sigma'_{32} & \sigma'_{33} \end{bmatrix} = \begin{bmatrix} a_{11} & a_{12} & a_{13} \\ a_{21} & a_{22} & a_{23} \\ a_{31} & a_{32} & a_{33} \end{bmatrix} \begin{bmatrix} \sigma_{11} & \sigma_{12} & \sigma_{13} \\ \sigma_{21} & \sigma_{22} & \sigma_{23} \\ \sigma_{31} & \sigma_{32} & \sigma_{33} \end{bmatrix} \begin{bmatrix} a_{11} & a_{21} & a_{31} \\ a_{12} & a_{22} & a_{32} \\ a_{13} & a_{23} & a_{33} \end{bmatrix} .$$

[7]

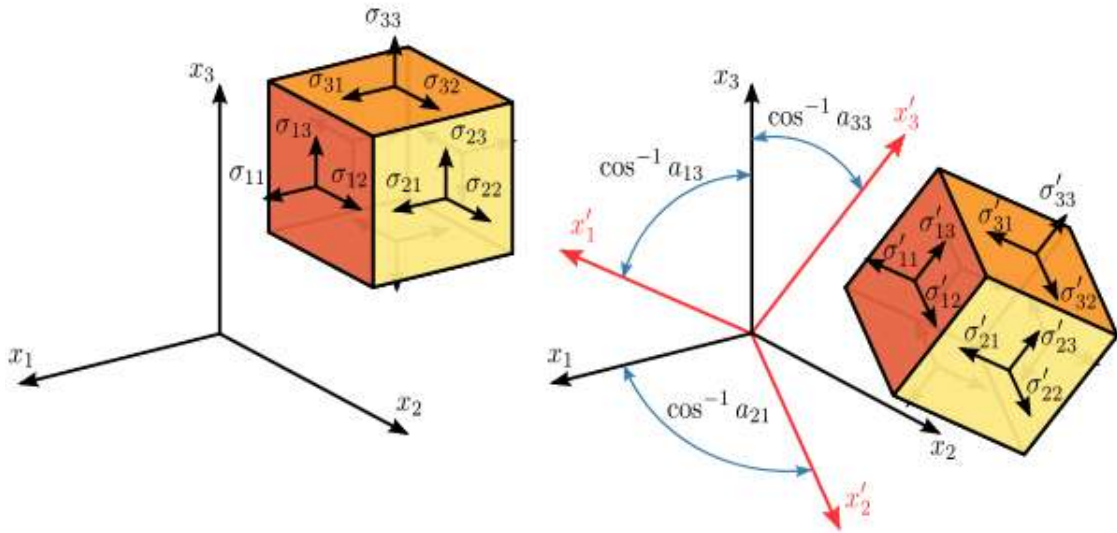


Figure – 3.6 Conversion of Stress Tensor

[15]

On simplifying it becomes:-

$$\sigma'_{11} = a_{11}^2\sigma_{11} + a_{12}^2\sigma_{22} + a_{13}^2\sigma_{33} + 2a_{11}a_{12}\sigma_{12} + 2a_{11}a_{13}\sigma_{13} + 2a_{12}a_{13}\sigma_{23},$$

$$\sigma'_{22} = a_{21}^2\sigma_{11} + a_{22}^2\sigma_{22} + a_{23}^2\sigma_{33} + 2a_{21}a_{22}\sigma_{12} + 2a_{21}a_{23}\sigma_{13} + 2a_{22}a_{23}\sigma_{23},$$

$$\sigma'_{33} = a_{31}^2\sigma_{11} + a_{32}^2\sigma_{22} + a_{33}^2\sigma_{33} + 2a_{31}a_{32}\sigma_{12} + 2a_{31}a_{33}\sigma_{13} + 2a_{32}a_{33}\sigma_{23},$$

$$\begin{aligned}
\sigma'_{12} &= a_{11}a_{21}\sigma_{11} + a_{12}a_{22}\sigma_{22} + a_{13}a_{23}\sigma_{33} \\
&\quad + (a_{11}a_{22} + a_{12}a_{21})\sigma_{12} + (a_{12}a_{23} + a_{13}a_{22})\sigma_{23} + (a_{11}a_{23} + a_{13}a_{21})\sigma_{13}, \\
\sigma'_{23} &= a_{21}a_{31}\sigma_{11} + a_{22}a_{32}\sigma_{22} + a_{23}a_{33}\sigma_{33} \\
&\quad + (a_{21}a_{32} + a_{22}a_{31})\sigma_{12} + (a_{22}a_{33} + a_{23}a_{32})\sigma_{23} + (a_{21}a_{33} + a_{23}a_{31})\sigma_{13}, \\
\sigma'_{13} &= a_{11}a_{31}\sigma_{11} + a_{12}a_{32}\sigma_{22} + a_{13}a_{33}\sigma_{33} \\
&\quad + (a_{11}a_{32} + a_{12}a_{31})\sigma_{12} + (a_{12}a_{33} + a_{13}a_{32})\sigma_{23} + (a_{11}a_{33} + a_{13}a_{31})\sigma_{13}.
\end{aligned}$$

Conversion of stresses is graphically represented by the Mohr circle.

### 3.13 PERPENDICULAR AND SHEAR STRESSES

The value of the component of perpendicular stress  $\sigma_n$  of any stress vector  $\mathbf{T}^{(\mathbf{n})}$  acting on an arbitrary plane with perpendicular vector  $\mathbf{n}$  at a given point, in terms of the components  $\sigma_{ij}$  of the stress tensor  $\boldsymbol{\sigma}$ , is the dot product of the stress vector and the perpendicular vector:

$$\begin{aligned}
\sigma_n &= \mathbf{T}^{(\mathbf{n})} \cdot \mathbf{n} \\
&= T_i^{(\mathbf{n})} n_i \\
&= \sigma_{ij} n_i n_j.
\end{aligned}$$

The amount of the shear stress component  $\tau_n$ , acting in the plane spanned by the two vectors  $\mathbf{T}^{(\mathbf{n})}$  and  $\mathbf{n}$ , can then be found using the Pythagorean hypothesis:

$$\begin{aligned}
\tau_n &= \sqrt{(T^{(\mathbf{n})})^2 - \sigma_n^2} \\
&= \sqrt{T_i^{(\mathbf{n})} T_i^{(\mathbf{n})} - \sigma_n^2},
\end{aligned}$$

Where

$$(T^{(\mathbf{n})})^2 = T_i^{(\mathbf{n})} T_i^{(\mathbf{n})} = (\sigma_{ij} n_j) (\sigma_{ik} n_k) = \sigma_{ij} \sigma_{ik} n_j n_k.$$

### 3.14 MAXIMUM AND MINIMUM SHEAR STRESSES

The maximum shear stress or the maximum principal shear stress equal to one-half the difference between the largest and smallest principal stresses, This stress acts on plane which bisects the angle between the largest of the greatest and smallest principal stresses i.e direction of shear stress is at an angle of  $45^\circ$  from the principal stress planes. The maximum shear stress is written as,

$$\tau_{\max} = \frac{1}{2} |\sigma_{\max} - \sigma_{\min}| \quad [13] \text{ and suppose that}$$

Assuming  $\sigma_1 \geq \sigma_2 \geq \sigma_3$  then we can calculate  $\tau_{\max}$  which is

$$\tau_{\max} = \frac{1}{2} |\sigma_1 - \sigma_3|$$

The stress component which is perpendicular on the plane for the most shear stress will not be zero and given by relation:-

$$\sigma_n = \frac{1}{2} (\sigma_1 + \sigma_3)$$

### 3.15 STRESS DEVIATOR TENSOR

The stress tensor  $\sigma_{ij}$  can be written as sum of two other stress tensors:

- One of them is mean hydrostatic tensor or called volumetric stress tensor or mean perpendicular stress tensor,  $p\delta_{ij}$ , which tends to affect and cause changes on the volume of body under stress and
- The other component called deviator stress tensor the stress deviator tensor,  $s_{ij}$ , which tends to distort it.

So:

$$\sigma_{ij} = s_{ij} + p\delta_{ij},$$

where  $p$  is the mean stress given by

$$p = \frac{\sigma_{kk}}{3} = \frac{\sigma_{11} + \sigma_{22} + \sigma_{33}}{3} = \frac{1}{3} I_1.$$

Here it should be noted that difference of conversion in solid mechanics. Solid mechanics describes it as negative 1/3 of trace of stress tensor.

The deviatoric stress tensor is the difference of the hydrostatic stress tensor and the stress tensor:

$$s_{ij} = \sigma_{ij} - \frac{\sigma_{kk}}{3}\delta_{ij},$$

$$\begin{bmatrix} s_{11} & s_{12} & s_{13} \\ s_{21} & s_{22} & s_{23} \\ s_{31} & s_{32} & s_{33} \end{bmatrix} = \begin{bmatrix} \sigma_{11} & \sigma_{12} & \sigma_{13} \\ \sigma_{21} & \sigma_{22} & \sigma_{23} \\ \sigma_{31} & \sigma_{32} & \sigma_{33} \end{bmatrix} - \begin{bmatrix} p & 0 & 0 \\ 0 & p & 0 \\ 0 & 0 & p \end{bmatrix}$$

$$= \begin{bmatrix} \sigma_{11} - p & \sigma_{12} & \sigma_{13} \\ \sigma_{21} & \sigma_{22} - p & \sigma_{23} \\ \sigma_{31} & \sigma_{32} & \sigma_{33} - p \end{bmatrix}. \quad [13]$$

### 3.16 INVARIANTS OF THE STRESS DEVIATOR TENSOR

As it is a second order tensor, the stress deviator tensor also has a set of invariants, which can be obtained using the same procedure utilized to calculate the invariants of the stress tensor. It should be noted that the principal directions of the stress deviator tensor  $s_{ij}$  and the principal directions of the stress tensor  $\sigma_{ij}$  are same. Therefore, the relation is [1]:

$$|s_{ij} - \lambda\delta_{ij}| = \lambda^3 - J_1\lambda^2 - J_2\lambda - J_3 = 0,$$

Where  $J_1$ ,  $J_2$  and  $J_3$  are called the first, second, and third deviator stress invariants, respectively. These are invariant because they do not change due to change of coordinate system. These deviatoric stress invariants can be expressed to be a function of the components of  $s_{ij}$  or its principal values  $s_1, s_2$ , and  $s_3$ , or alternatively, to be a function of  $\sigma_{ij}$  or its principal values  $\sigma_1, \sigma_2$ , and  $\sigma_3$ . Thus,

$$\begin{aligned}
J_1 &= s_{kk} = 0, \\
J_2 &= \frac{1}{2} s_{ij} s_{ji} \\
&= -s_1 s_2 - s_2 s_3 - s_3 s_1 \\
&= \frac{1}{6} [(\sigma_{11} - \sigma_{22})^2 + (\sigma_{22} - \sigma_{33})^2 + (\sigma_{33} - \sigma_{11})^2] + \sigma_{12}^2 + \sigma_{23}^2 + \sigma_{31}^2 \\
&= \frac{1}{6} [(\sigma_1 - \sigma_2)^2 + (\sigma_2 - \sigma_3)^2 + (\sigma_3 - \sigma_1)^2] \\
&= \frac{1}{3} I_1^2 - I_2, \\
J_3 &= \det(s_{ij}) \\
&= \frac{1}{3} s_{ij} s_{jk} s_{ki} \\
&= s_1 s_2 s_3 \\
&= \frac{2}{27} I_1^3 - \frac{1}{3} I_1 I_2 + I_3.
\end{aligned}$$

Because  $s_{kk} = 0$ , this means that it is in pure shear state.

A Von Mises stress [1] is utilized in solid mechanics. Which is defined as:-

$$_{[1]} \sigma_e = \sqrt{3 J_2} = \sqrt{\frac{1}{2} [(\sigma_1 - \sigma_2)^2 + (\sigma_2 - \sigma_3)^2 + (\sigma_3 - \sigma_1)^2]}.$$

### 3.17 OCTAHEDRAL STRESSES

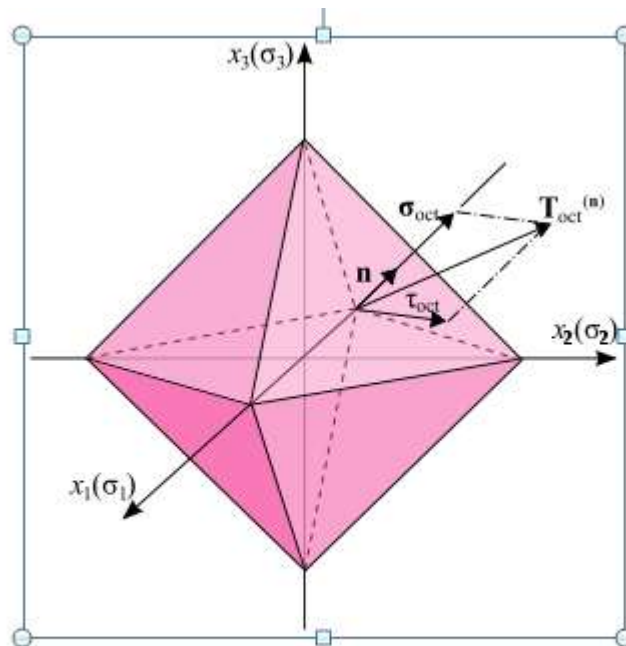


Figure – 3.7 Octahedral Stress Planes

Figure 3.7 [16] illustrates the plane of octahedral stresses.

Considering the principal directions to be the coordinate axes, a plane whose perpendicular vector makes equal angles with each of the principal axes (i.e. having direction cosines equal to  $|1/\sqrt{3}|$ ) is called an octahedral plane. It has eight octahedral planes. It has a perpendicular component and shear component of the stress tensor on these planes are called octahedral perpendicular stress  $\sigma_{\text{oct}}$  and octahedral shear stress  $\tau_{\text{oct}}$ , respectively.

Knowing that the stress tensor of point O in the principal axes is

$$\sigma_{ij} = \begin{bmatrix} \sigma_1 & 0 & 0 \\ 0 & \sigma_2 & 0 \\ 0 & 0 & \sigma_3 \end{bmatrix}_{[13]}$$

the stress vector on an octahedral plane is expressed as:-

$$\begin{aligned} \mathbf{T}_{\text{oct}}^{(\mathbf{n})} &= \sigma_{ij} n_i \mathbf{e}_j \\ &= \sigma_1 n_1 \mathbf{e}_1 + \sigma_2 n_2 \mathbf{e}_2 + \sigma_3 n_3 \mathbf{e}_3 \\ &= \frac{1}{\sqrt{3}} (\sigma_1 \mathbf{e}_1 + \sigma_2 \mathbf{e}_2 + \sigma_3 \mathbf{e}_3) \end{aligned}$$

The component of the stress vector which is perpendicular at point O linked with the octahedral plane is described as:-

$$\begin{aligned} \sigma_{\text{oct}} &= T_i^{(n)} n_i \\ &= \sigma_{ij} n_i n_j \\ &= \sigma_1 n_1 n_1 + \sigma_2 n_2 n_2 + \sigma_3 n_3 n_3 \\ &= \frac{1}{3} (\sigma_1 + \sigma_2 + \sigma_3) = \frac{1}{3} I_1 \end{aligned}$$

It is also called the mean perpendicular stress or hydrostatic stress. This value is equal in all eight octahedral planes. The shear stress on the octahedral plane will now be calculated as:-

$$\begin{aligned} \tau_{\text{oct}} &= \sqrt{T_i^{(n)} T_i^{(n)} - \sigma_{\text{oct}}^2} \\ &= \left[ \frac{1}{3} (\sigma_1^2 + \sigma_2^2 + \sigma_3^2) - \frac{1}{9} (\sigma_1 + \sigma_2 + \sigma_3)^2 \right]^{1/2} \\ &= \frac{1}{3} \left[ (\sigma_1 - \sigma_2)^2 + (\sigma_2 - \sigma_3)^2 + (\sigma_3 - \sigma_1)^2 \right]^{1/2} = \frac{1}{3} \sqrt{2I_1^2 - 6I_2} = \sqrt{\frac{2}{3} J_2} \end{aligned}$$

### 3.18 STRAIN

A strain is a normalized measure of bend/twist (deformation) showing the movement amongst discrete minute parts in the body relative to a reference length. A general bend/twist of a body can be expressed in the shape  $\mathbf{x} = \mathbf{F}(\mathbf{X})$  where  $\mathbf{X}$  is the reference position of material points in the body. Such a measure does not distinguish between stiff body motions and changes in shape (and size) of the body. A bend/twist has units of length.

In mathematical expression it can be expressed as:

$$\boldsymbol{\epsilon} \doteq \frac{\partial}{\partial \mathbf{X}} (\mathbf{x} - \mathbf{X}) = \frac{\partial \mathbf{F}}{\partial \mathbf{X}} - \mathbf{1} \quad .[2]$$

Strains have no dimensions and are usually expressed as fraction (of decimal) or %age. Strains measure how much a given bend/twist differs locally from a stiff-body bend/twist.

A strain is in general a tensor quantity. Physical insight into strains can be gained by observing that a given strain can be resolved into perpendicular and shear components. The amount of stretch or compression along a material line elements or fibers is the perpendicular strain, and the amount of distortion associated with the sliding of plane layers over each other is the shear strain, within a deforming body. This could be applied by elongation, shortening, or volume changes, or angular distortion.

The state of strain at material point of a continuum body is described as total displacement or deformation in the fibres or lines of material. The perpendicular strain, which pass through that point and also the totality of all the changes in the angle between pairs of lines initially perpendicular to each other, the shear strain, radiates from this point.

In the length of material is increase then, the perpendicular strain is called tensile strain, otherwise, if there is reduction or suppression in the length of the material line, this is compressive strain.



# CHAPTER 4

## AVLB PARTS MODELLING IN PROE/ANSYS

To carry out the analysis of critical parts, each and every component was modeled in Proe. This step was main phase of the research as any errors in the model or flaws of even a small dimension could have generated errors. In the beginning a number of errors were observed but they were identified and correction was applied to reach to correct loading / constraint applications etc. The modeling in ANSYS/ Mechanical is based on FEM [17]

### 4.1 MODELLING IN PROE/ANSYS

This is one of the techniques available to engineers to carryout design analysis. It has embedded features to solve complex differential equations and give results. This soft ware was used to prepare the model for analysis. Completed description of each and every step involved is stated in under mentioned paragraphs. Graphical and numerical results can be used to assess stresses and strains in the light of different theories.

### 4.2 STRESS ANALYSIS OF SOLIDS

To carryout analysis of any solid in 3D Mechanical and ANSYS applications were used. For analysis of solid structures Mechanical can be used to directly apply its analysis techniques, in this case Proe designs/drawings were used. The given features were used to make the component similar to the actual conditions used in AVLB for taking load. Where as in ANSYS, modeling is difficult, but any solid can be modeled easily in Proe and make its \*.igs or \*.sat file by saving them as solids (not surfaces).

### 4.3 TECHNIQUES OF ANALYZING SOLIDS PIN PROE

#### 4.3.1 Make a Part (Pin)

Part i.e. pin was made by using Proe. So available drawings were converted / transformed into Proe parts and files were saved while requisite dimensions were maintained. Dimensions were in mm. The parts were drawn as solids where as a hollow pin could have given different result.

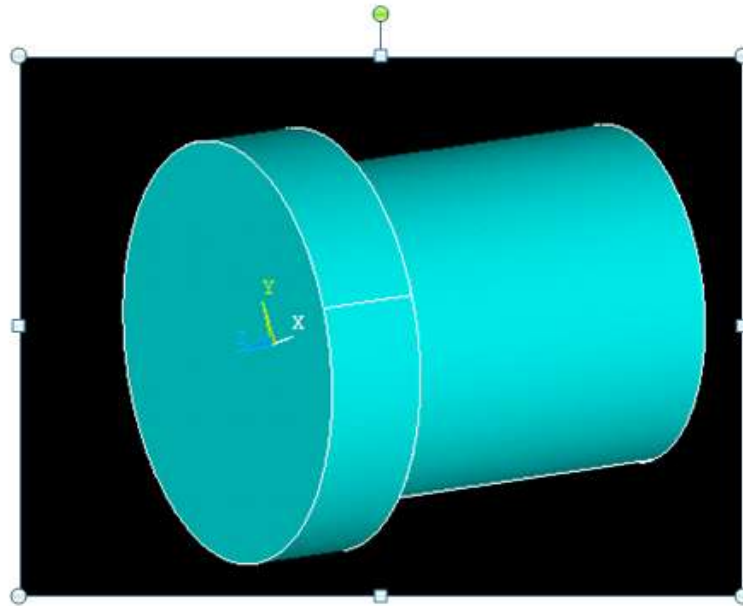


**Figure – 4.1 Pin/Part of Load Taking Structure**

#### **4.3.2 Analysis in Mechanics**

Now a model was created in FEM. Mechanics is used to carry out analysis of solid. By using the side tool commands required model was constructed to carryout analysis. World coordinate system (WCS) can be easily adopted. However, other coordinate system was also available and could be used if desired. Analysis of solid as part of structure was to be carried out therefore, it was selected as solid.

#### **4.3.3 Defining Constraints**

Constraints were applied keeping in view the application of forces and constraints available in the actual model where the solid had to be used. Number of constraints could vary for each type of analysis to analysis. Now constraints could have been applied on points, surfaces, edges, curves etc. Degree of freedom as per the requirements of analysis in X, Y, Z axis direction or on rotation about X, Y,Z axis was applied to restrict move of component during application of loads.

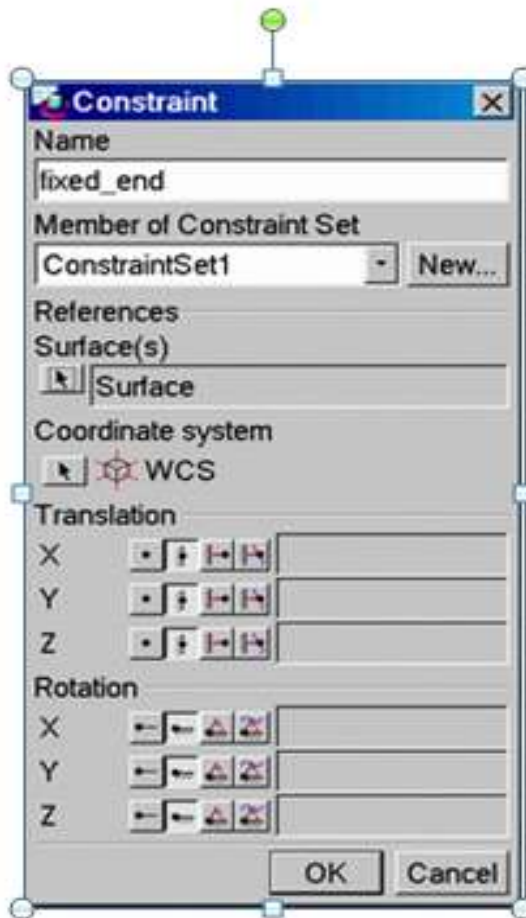


**Figure – 4.2 Application of Constraints**

#### 4.3.4 Application of Forces/Loads

Loads or forces could be applied in any direction or even moments could be applied. A FEM model can have any number of different load sets. Forces could have acted in any direction. Forces were applied in the given direction +ve or -ve. Here the force/moment units have to be consistent. Unit of force was kept as N and stress was in MPa. The same is shown in figure 4.3 and 4.4.

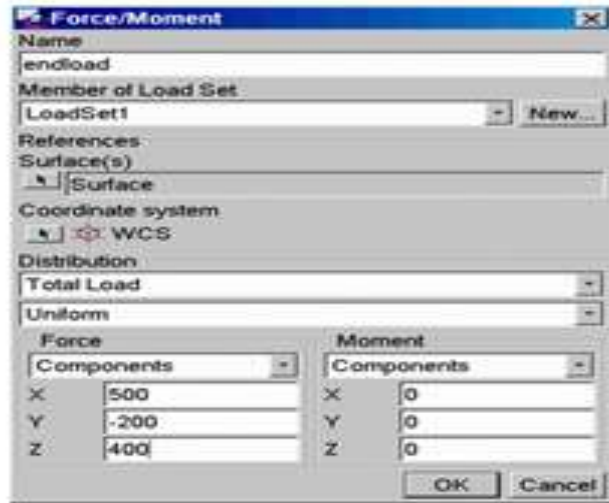


**Figure – 4.3 Application of Forces**

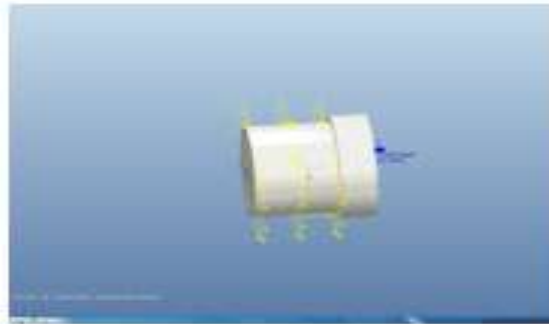


**Figure – 4.4 Application of Forces on Pin**

#### 4.3.5 Material Properties Assignment

A number of materials are available in the library provided by the Mechanica. If a material of similar properties is available in material library then it can be selected directly, otherwise we can give material properties of our choice which include the maximum yield strength of material, maximum tensile strength, Young's modulus, poisson's ratio, and units of these quantities should remain consistent. Here material of desired properties was not available in the material library. To prepare the model, material was assigned as per the required material properties.

#### 4.3.6 Defining the Type of Analysis

Type of analysis is specified which can be static, modal, transient or harmonic etc [21]. The analysis carried out was static analysis. The results were of different types. These

were of deformed shape, Von Mises stress, principal stress, max shear stress or animation of application of forces/deflection were available and plotted.



**Figure – 4.5 Defining Type of Analysis**

#### 4.3.7 Creating the Mesh on Object

To carryout analysis in FEM, a mesh has to be created meshing of component is required prior to start of analysis. For this option available in the menu was used. A default image of mesh is shown in figure 4.6. Mechanica does not provide very fine mesh. How ever results were also different for different mesh refinements.

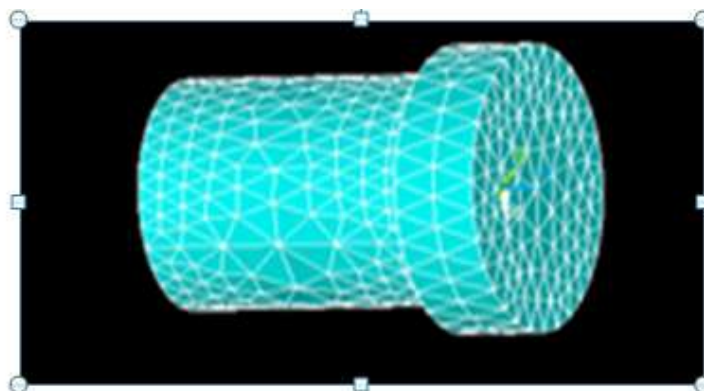


**Figure – 4.6 Meshing Application**

#### 4.3.8 Improving the Mesh

In the mesh command 'Control' option can be selected to allow to carryout refinement of mesh on desired surfaces like some hole or some joint etc. So keeping in view the critical area meshing was applied on Pin.

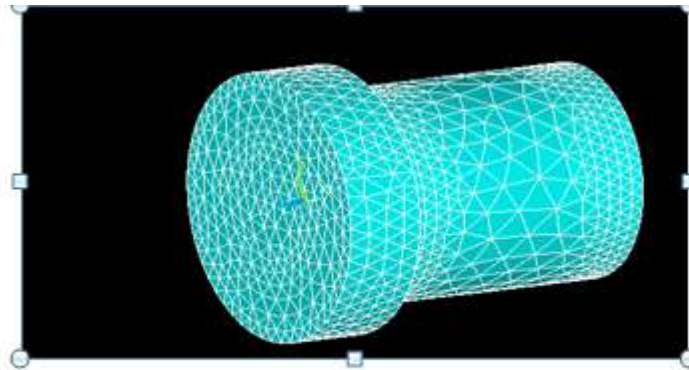


**Figure – 4.7 Refinement of Mesh**

#### 4.3.9 Creating the Output file of Work

Different file name/file folder was created each time to carryout analysis of each part. Different options were available to view the results in animations, displacement, Von Mises or principal stresses, etc.

#### 4.3.10 Analysis of Solids/Parts in ANSYS

Analysis of solids or parts was also carried out in ANSYS. To model a 3D solid in ANSYS is time consuming, however, solid parts were easily modeled by importing Proe parts or \*.sat or \*.igs files.

#### 4.3.11 Designation of ANSYS Title

Command (utility menu> File change title) was given for defining the title. This title is used for graphics displays etc. So the title of each job was kept separate just to refer back for viewing the results.

#### 4.3.12 Units Identification

ANSYS does not assume a system of units for analysis, except for magnetic field analysis. The system of units used was in mm for displacement/dimension and N for forces, however, the system of units adopted must be consistent.

#### 4.3.13 Elements Type

ANSYS elementary library contains more than 150 different types of materials/elements. A number of element categories are given in the library of materials from where they were assigned to the job. Brick quad 45 Solid was selected as the element for the model/job.

#### 4.3.14 Elements Real Constants

There are real constants or properties which depend on type of element in use. It includes cross sectional area, moment of inertia of beam/solid, deflection constant (due to shear) etc. Command is Mainmenu>preprocessor>modeling>create>elements>elem attributes. So this command was just required for elements real constants.

#### 4.3.15 Material Properties

Most elements have their material property which is selected on the basis of its application. These properties can be linear or non linear. In these analyses material used was linear, isotropic material. Different plots were required for various uses depending upon their application. Some of them are as under:-

MPLOT It gives material properties plot.

K PLOT It gives key points plot

PLOT It gives lines plot

N Plot It give plot of nodes.

#### 4.3.16 Considerations for a Structural Analysis

Following considerations required attention, input values of elastic materials i.e. elastic modulus of 207 KN/ mm square, poisson's ratio of 0.33 were selected for armour steel.

#### 4.3.17 Meshing of Solid

Meshing can be performed by the ANSYS default, which can provide adequate solution for analysis. However, mesh control was used for specific surfaces or areas of the solid. The ANSYS mesh tool was used by following command.

Mainmenu>Preprocessor> Meshing>Meshtool

Following functions were available via mesh tool to include;-

- a. Smart mesh size
- b. Element size control
- c. Specifying element shape
- d. Specifying mesh type (mapped)
- e. Meshing solid entities
- f. Clearing mesh
- g. Refining mesh

#### 4.3.17 Solution of Model/Solid Analysis

In this phase solution of model was done where following actions were adopted:-

##### 4.3.17.1 Application of Constraints

In this method constraints applied on the model to simulate the actual condition of the component. Command used was Mainmenu>preprocessor>solution>defineloads>apply>displacement on areas or nodes or lines. The area of pin to be constrained was selected to apply constraint.

##### 4.3.17.2 Application of Forces

Forces were applied as per the actual conditions in the X, Y or Z directions as per world coordinate system. Units of forces should be consistent, command is Mainmenu>preprocessor>solution>defineloads>apply>forces/moments on lines or nodes or elements. Forces were applied on nodes e.g. are as following

Total load  $F=70$  Ton

Angle of application  $=20^\circ$

$$F_Y = F \sin 20^\circ \quad F_X = F \cos 20^\circ$$

The load was distributed on selected number of nodes e.g. 300 and computed for  $F_x/300$  or  $F_y/300$ .



#### 4.3.17.3 Analysis Type

A number of different types of analysis could be performed e.g. is given below. Scope of this research was limited to Static analysis.

- a. Static
- b. Modal
- c. Harmonic
- d. Transient
- e. Spectrum
- f. Eigen Buckling
- g. Sub structuring

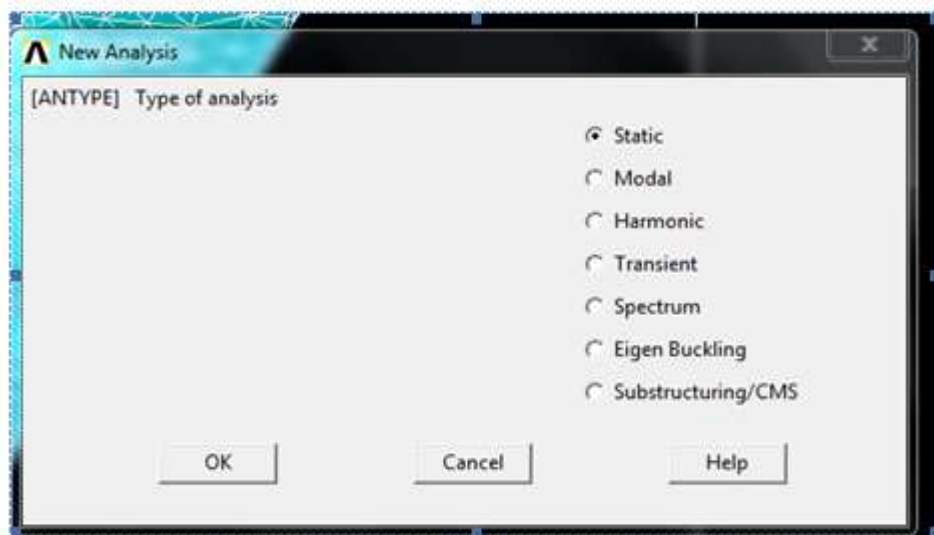


Figure- 4.8 Type of Analysis

#### 4.2.17.4 Solution of LS

Command of solving the LS is as following Mainmenu>preprocessor>solution> solve> current LS. This command was utilized to solve the load system. Another window appeared which showed “Solution is done”.

#### 4.2.22 Display of Results

The desired results after solution were stored in the data base, which were viewed by

using the graphic displays and tabular listings. Graphic representations of results included following:-

- a. Contour displays for Von Mises stress, principal stress etc
- b. Deformed shape displays were used to analyze the component behavior
- c. Vector displays
- d. Path plots
- e. Reaction force displays
- f. Particle flow traces

Commands of some of the above mentioned solutions are as under, these were used just for display of results.

Mainmenu>Generalpostproc>Plotresults>contourplot>nodalsolution or

PLNSOL

Mainmenu>Generalpostproc>Plotresults>contourplot>Plotelementsolu or

PLESOL

Mainmenu>Generalpostproc>Plotresults>contourplot>elemtable or PLETAB

# CHAPTER 5

## RESULTS AND THEIR ANALYSIS

### 5. PROBLEM STATEMENT AND OBJECTIVES

The project assigned by MVRDE was to carry out the design analysis of the structure of carrier of the AVL B, so the following were the standards / steps involved in carrying out the analysis of the system.

- a. Problem was required to solve for static loading conditions only
- b. Drawing of main critical parts in Proe software
- c. Identification of critical parts, joints of launching system of bridge.
- d. Mathematical calculations of max load/moments of the bridge.
- e. Analysis of designed parts in Mechanica and ANSYS
- f. Confirmation of existing design or verdict on its failure/success
- g. Recommend the viable changes in the proposed design

#### 5.1 DESIGNS IN PROE

All drawings of AVL B available with MVRDE were converted into Proe. All measurement, dimensions etc were kept consistent in mm. MVRDE had already prepared drawings of most of the components of AVL B in Proe and a number of assemblies/sub assemblies were combined to prepare simulations.

#### 5.2 IDENTIFICATION OF CRITICAL PARTS

Most of the brackets, bracket plate, pins and hinges that were taking load of the bridge were identified as load taking parts. Their load assessment was anticipated by calculation of various loads in various phases at different angles and only analysis of critical parts was carried out. Forces were transformed into X and Y components with respect to direction of application of force.

For a load of 70 Tons, the calculations of forces are as under:-

Load= 70 Tons = 70,000 Kg

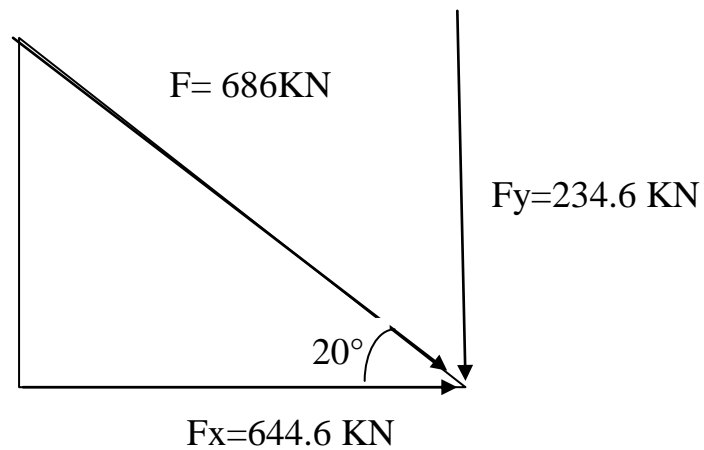
$$= 70000 \times 9.8 \text{ N}$$

$$= 686 \text{ KN}$$

$$F_Y = F \sin 20^\circ$$

$$F_X = F \cos 20^\circ$$

The Load distribution was also catered for in the application of forces. For example 4x brackets were taking the load, so the load of 70 Tons was divided by 4 for exact distribution of load.



<u>Data of Bridge/Hull/Material</u>	
▪ Weight of Bridge	10.8 tons
▪ Peak Load on the Bridge	60 tons
▪ Poisson's Ratio of Hull Material (Armour Steel)	0.33
▪ Modulus of Elasticity	207 Gpa
▪ Max Yield Strength	1000 Mpa
▪ Proposed Design Strength	70 tons

**Figure – 5.1 Data of Bridge/Hull Material**

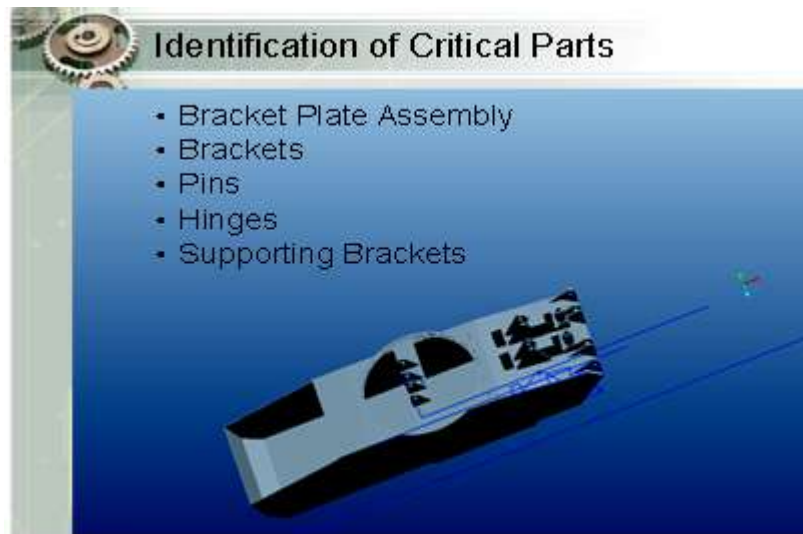


**Figure – 5.1.1 Hull Assembly Indicating Load Taking Parts**

### **5.3 CALCALATIONS OF MOMENTS**

Although the load of 10.8 tons was to be lifted by the main cylinders of the lifting mechanism but the load taking surface/brackets/pins were also to be subjected to moments. These moments were absorbed by distribution in a number of brackets which were taking the loads, however, following assumptions were made:-

- a. Intermediate hinges, were removed till the rotation point for calculation of moments, this was visualized for maximum moments, otherwise moments were on lower side.
- b. Combined effect was also catered for due to joints in the structure.
- c. System was analysed for max moment generated (68.8 Tons-m)

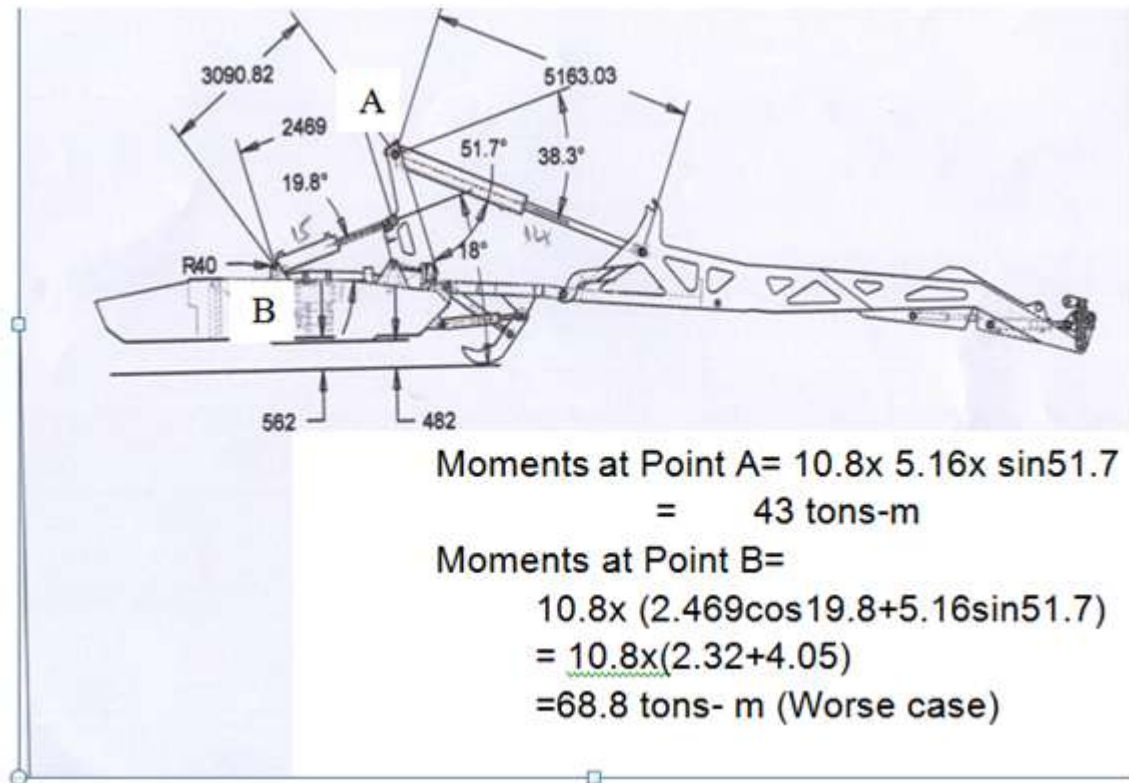


Figure 5.2 Angular Orientation of AVLB

#### 5.4 RESULTS ANALYSIS / DISCUSSION

Critical components parts were subjected to different loads/moment as already explained in chapter 4. However, they were separately analysed in Mechanica and ANSYS. All critical parts were given loads as per visualized pattern and results were obtained. Von Mises stress was kept as the failure criteria of the component. Maximum displacement and principal stresses were also kept in observation just to recognize the behavior of a part under the given loading conditions. The same components/parts were also analysed in ANSYS and there models were prepared as per actual models and availability of CPU resources.

These results were compared and recommendations were made. Passing components / parts and those parts which failed were also identified based on the failure analysis of components, alternates of failing components were prepared and designs were modified accordingly, and included in the recommendations. Complete details are shown in each figure, results are discussed below:-

### 5.4.1 BRACKET ANALYSIS IN MECHANICA

Analysis of bracket was carried out with following loading conditions:-

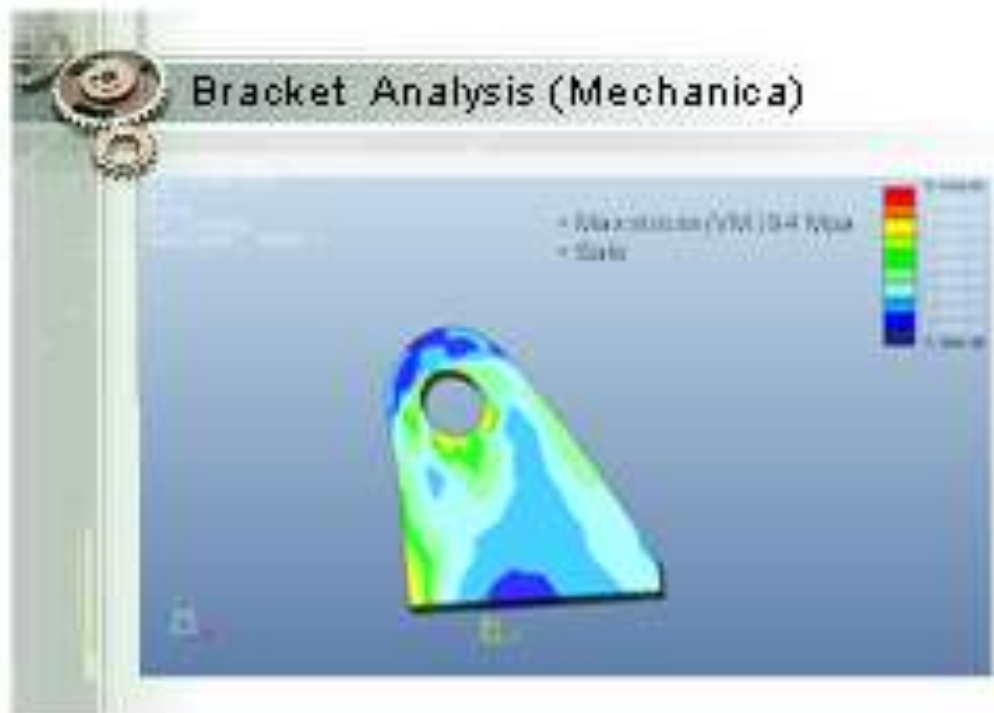
- a. Max Load = 70 Tones
- b. Components of load  $F_x=161$  KN  
and  $F_y = 58.6$  KN
- c. Material was armour steel with max yield strength of 1000 MPa and Poisson's ratio of 0.33
- d. Constraints were applied in the bottom surface/area of plate
- e. Material selection was structural, elastic, isotropic
- f. Mesh generation was course.



Figure - 5.3 Bracket Plate Analysis in Mechanica

### 5.4.2 PARTS RESPONSE TO STRESSES (MECHANICA)

After application of forces, the bracket assembly did not fail due to stresses as Von Mises stress was 94 MPa (9.4% of yield strength) and max displacement was 0.14 mm. The stress is much less than (1/10 of) yield strength. The same is shown in Figures 5.4 and 5.5.



**Figure - 5.4 Von Mises Stress on Bracket**

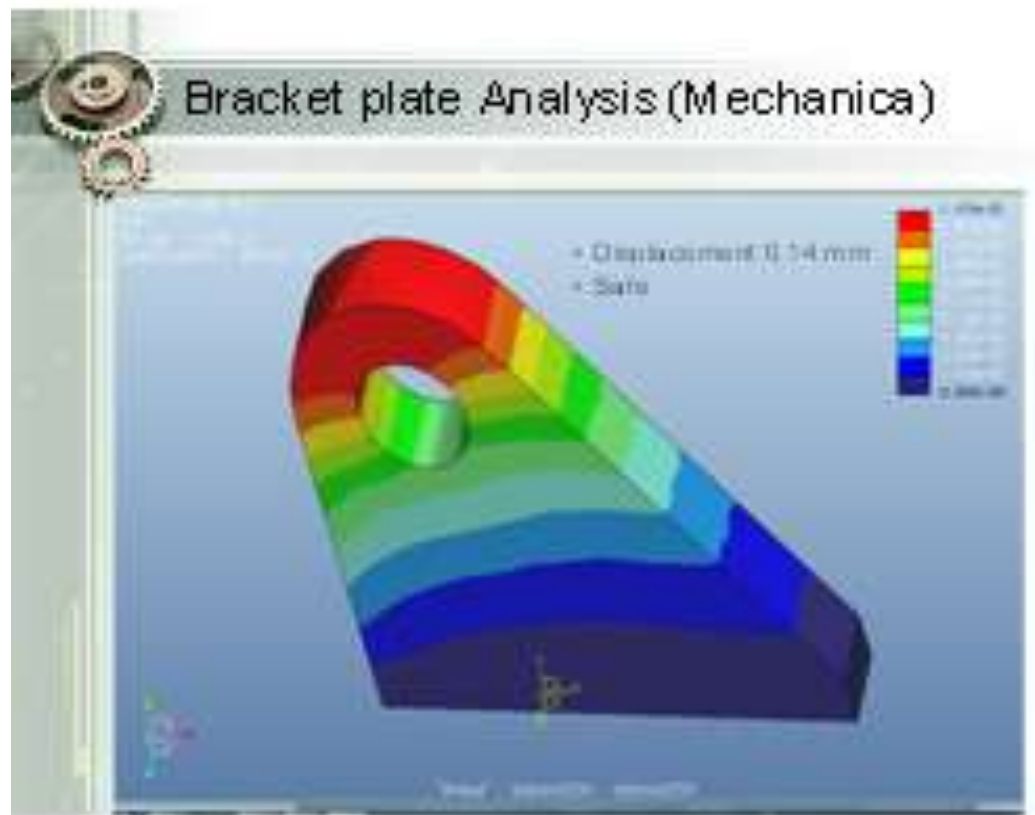


**Figure - 5.5 Bracket Displacement**



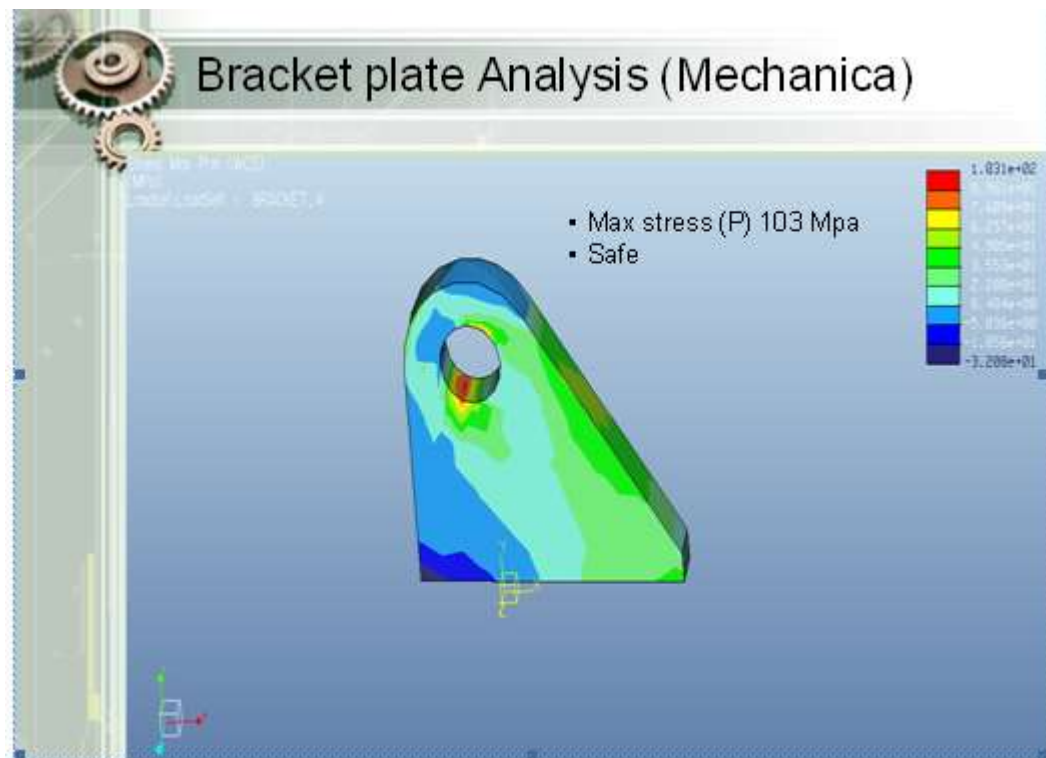


**Figure – 5.6 Bracket Under Max Principal Stress**

#### 5.4.3 BRACKET ANALYSIS IN ANSYS

Analysis of bracket was carried out with following loading conditions:-

- a. Max Load = 70 Tones
- b. Components of load  $F_x=161$  KN  
and  $F_y = 58.6$  KN, both  $F_x$  and  $F_y$  were divided by 4 (4 brackets)
- c. Material was armour steel with max yield strength of 1000 MPa and Poisson's ratio of 0.33
- d. Constraints were applied in the bottom surface/area of plate
- e. Material selection was structural, elastic, isotropic
- f. Mesh generation was smart.

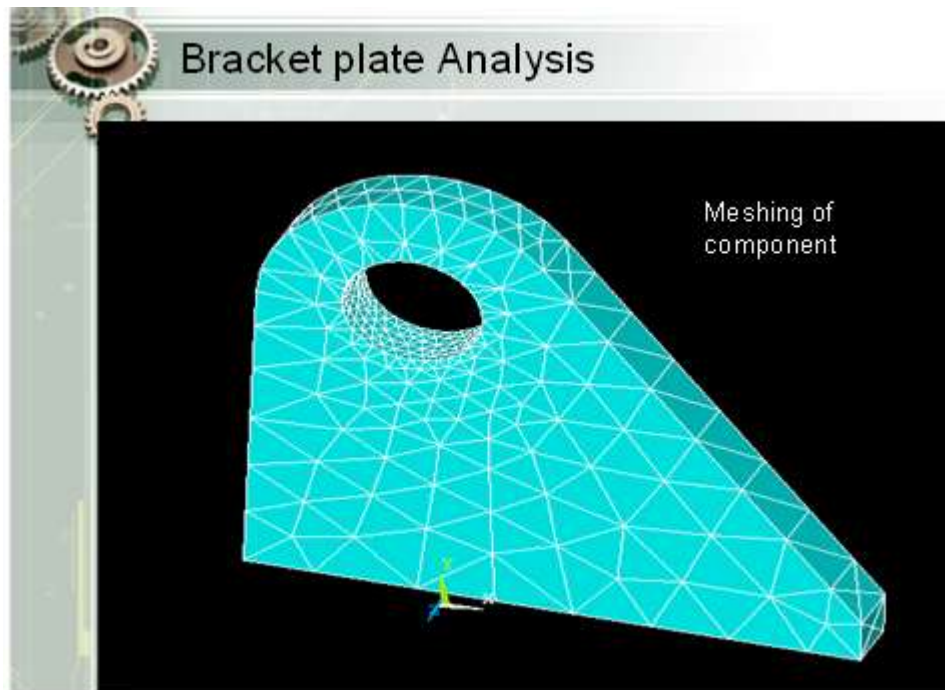


**Figure – 5.7 Mesh of Bracket**

#### 5.4.4 PARTS RESPONSE TO STRESSES

After application of forces, the bracket assembly did not fail due to stresses as Von Mises stress was 94 MPa (9.4% of yield strength) and max displacement was 0.11 mm. The stress is much less than (1/10 of) yield strength. The results are shown in figures 5.8 and 5.9.

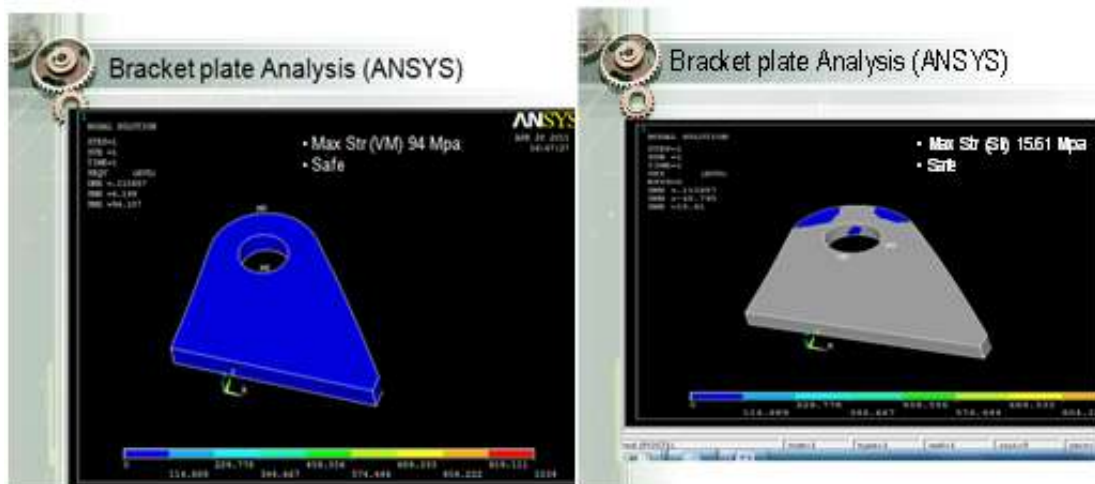


**Figure – 5.8 Von Mises Stress**

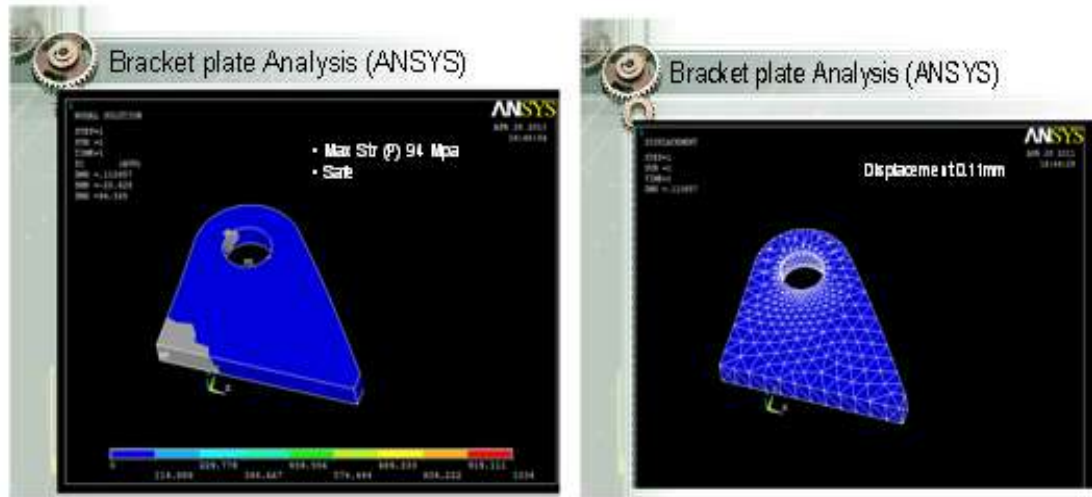


**Figure – 5.9 Max principal Stress in Bracket**

5.8

#### 5.4.5 COMPARISON OF RESULTS

Type	Mechanica	ANSYS	Remarks
Von Mises (MPa)	94	94	Equal in both cases
Max Principle (Mpa)	121	94	Mechanica showed more principal stress, error may be due to course mesh
Displacement (mm)	0.14	0.11	Almost equal

#### 5.4.6 CONCLUSION

Comparison shows that both the results are in conformation. Material is safe under the 70 Tons of static load.

#### 5.4.7 PIN'S ANALYSIS IN MECHANICA

Loading conditions and material properties and mesh caution is similar to paragraph 5.5. The load applied was Fx and Fy. However, constraints were applied on side surfaces of pins.

#### 5.4.8 PIN'S RESPONSE TO STRESSES

Pin's response is shown in figures 5.10, 5.11. The Pin has max principal of 14 Mpa. It is safe.

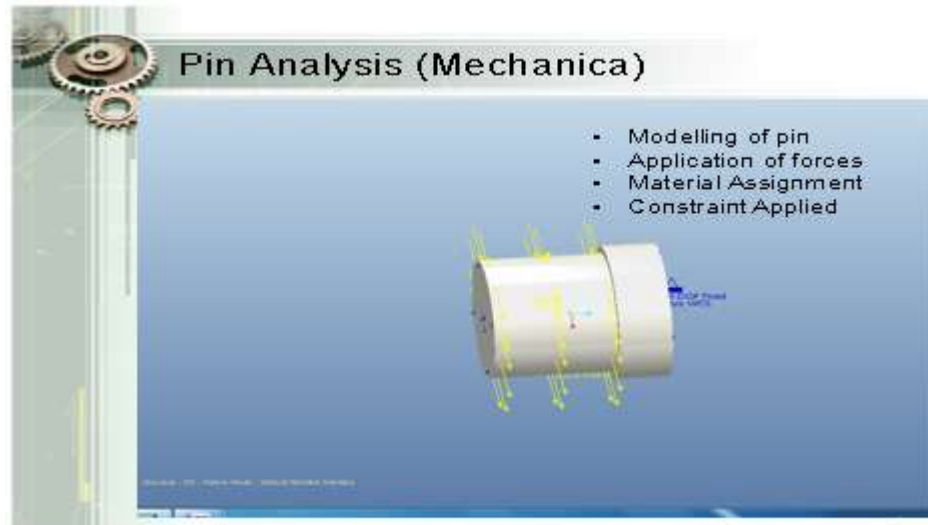


Figure – 5.10 Forces on Pin

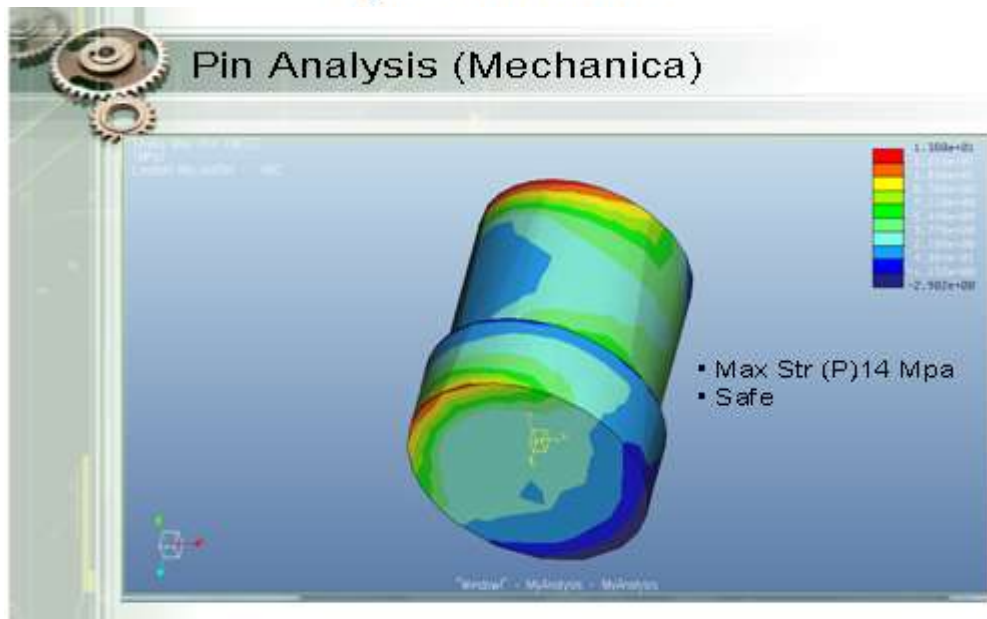
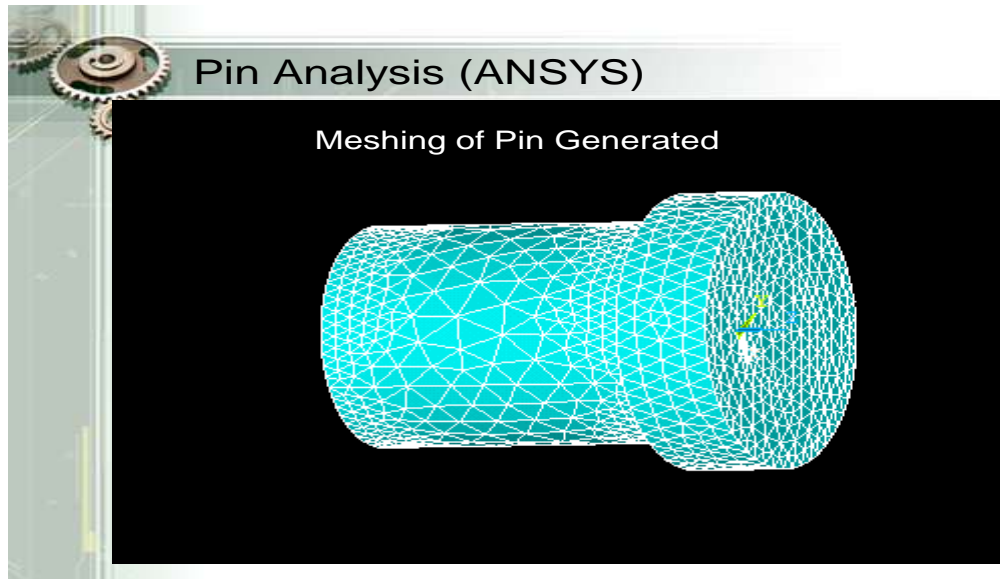


Figure – 5.11 Maximum Principal Stress on Pin

#### 5.4.9 PIN'S ANALYSIS IN ANSYS

Loading conditions and material were similar to conditions of pin in Mechanica. Constraints were applied on sides of pin. Meshing done was smart.



**Figure – 5.12 Pin with Mesh**

#### 5.4.10 PIN'S RESPONSE IN STRESS

It has max Von Mises stress of 87 MPa and displacement of 0.01 the pin is safe under the loading conditions.

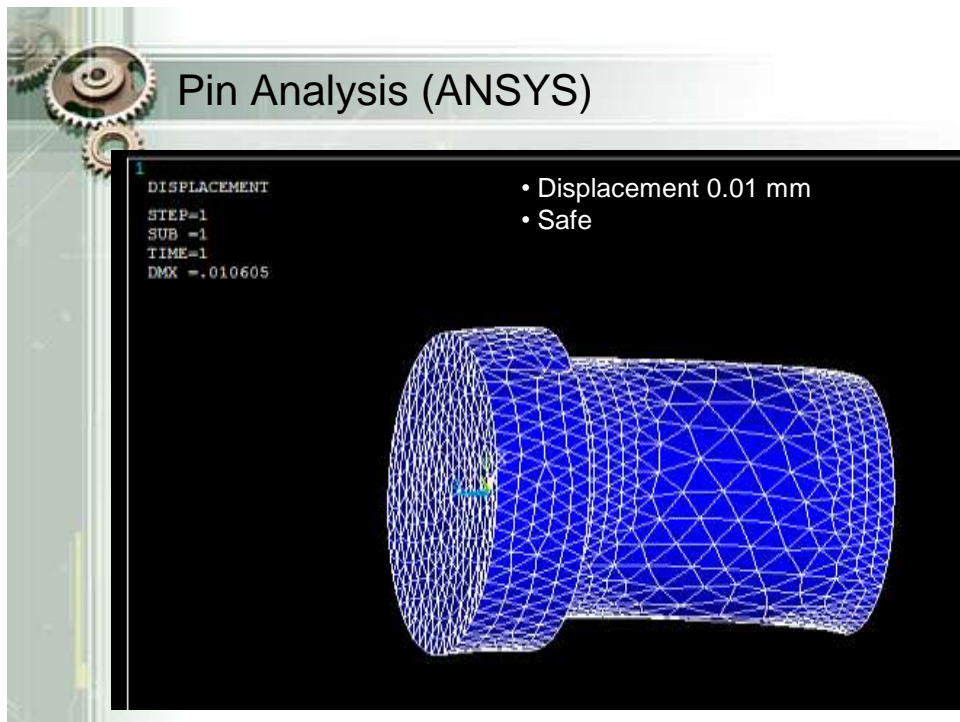


**Figure – 5.13 Pin displacement**

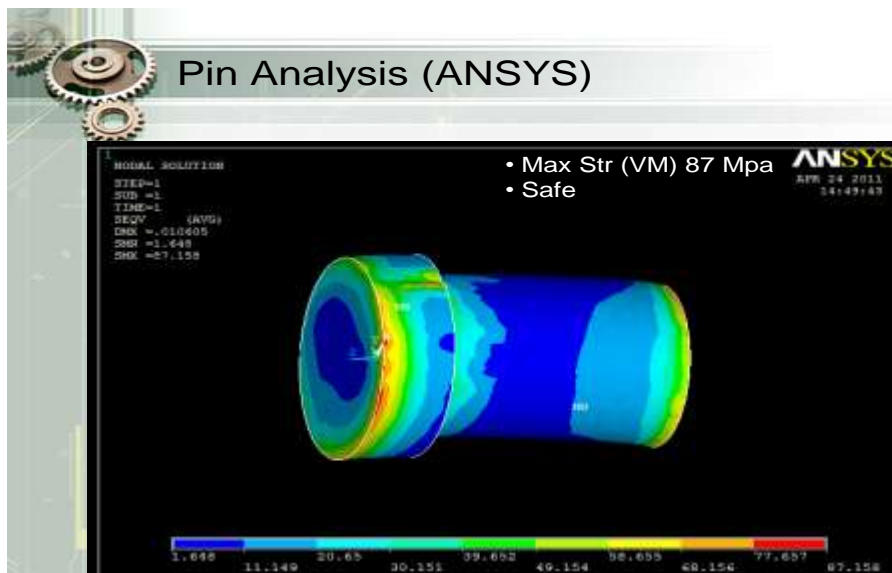


**Figure – 5.14**

#### 5.4.11 CONCLUSION

Comparison shows that both the results are in conformation. Material is safe under the 70 Tons of static load, stresses in ANSYS are higher side than Mechanical.

### 5.4.12 BRACKET PIN'S ANALYSIS IN MECHANICA

Bracket pin loading conditions same as per pin in Mechanica with coarse mesh.

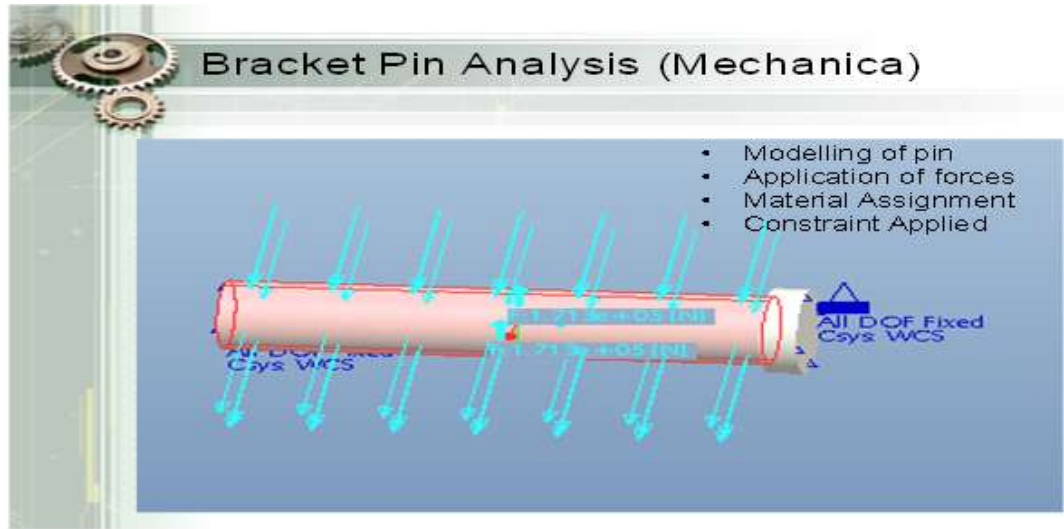


Figure – 5.15 Application of Forces on Pin

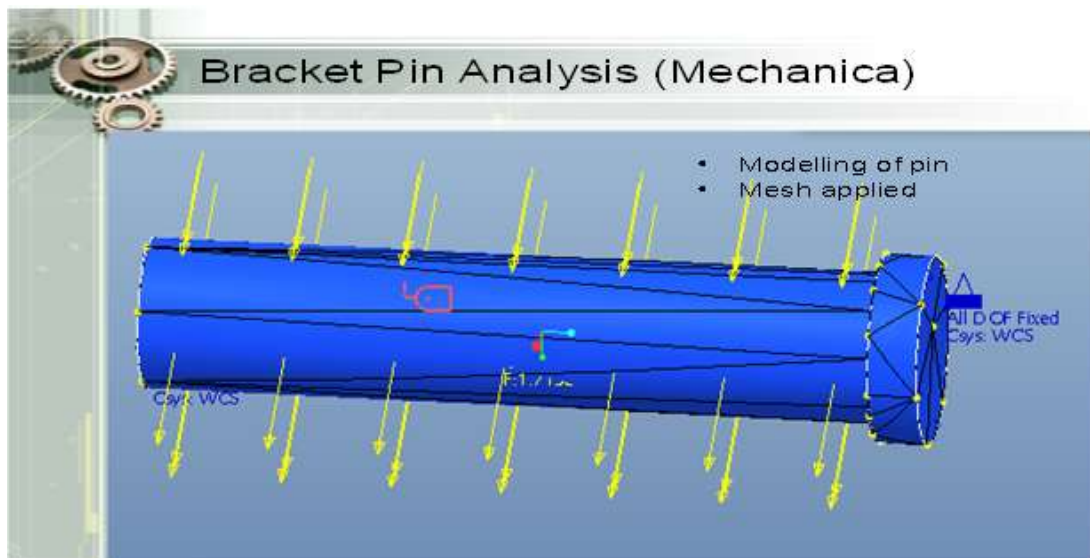


Figure – 5.16 Mesh of Pin

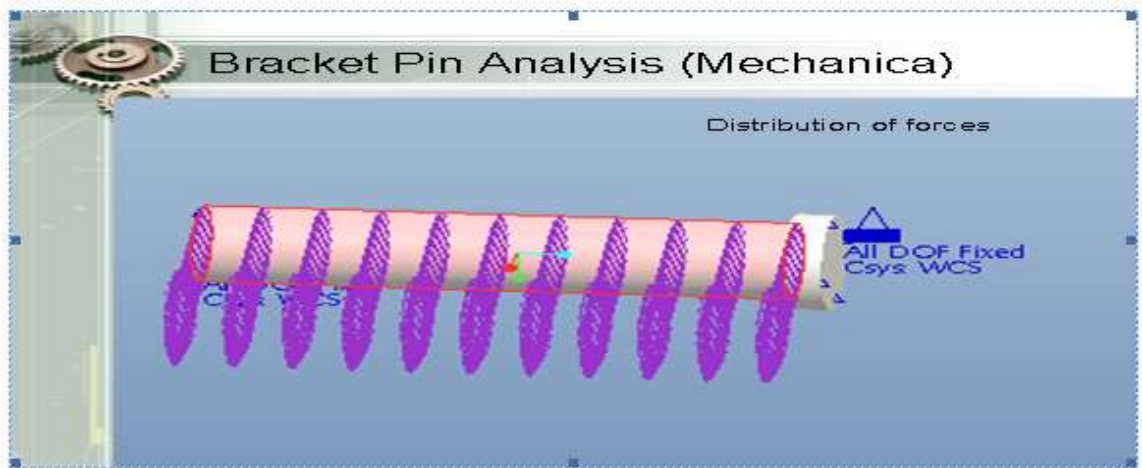


Figure – 5.17 Direction of Forces on Pin

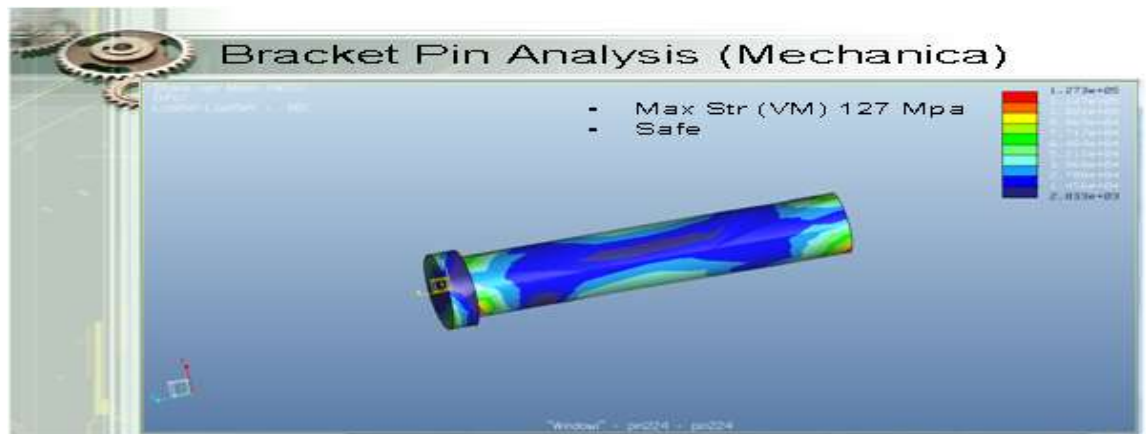


Figure – 5.18 Von Mises Stress on Pin

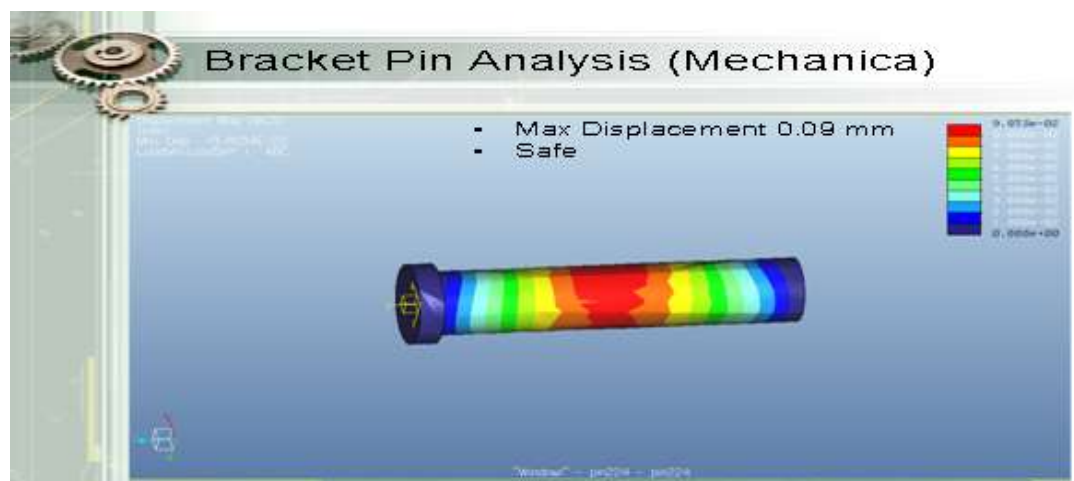


Figure – 5.19 Displacement on Pin



#### 5.4.13 BRACKET PIN'S RESPONSE IN STRESS

It has max Von Mises stress of 127 MPa and displacement of 0.09 mm the pin is safe under the loading conditions.

#### 5.4.14 BRACKET PIN'S ANALYSIS IN ANSYS

Bracket pin loading conditions are same as pin in Mechanica with smart mesh.

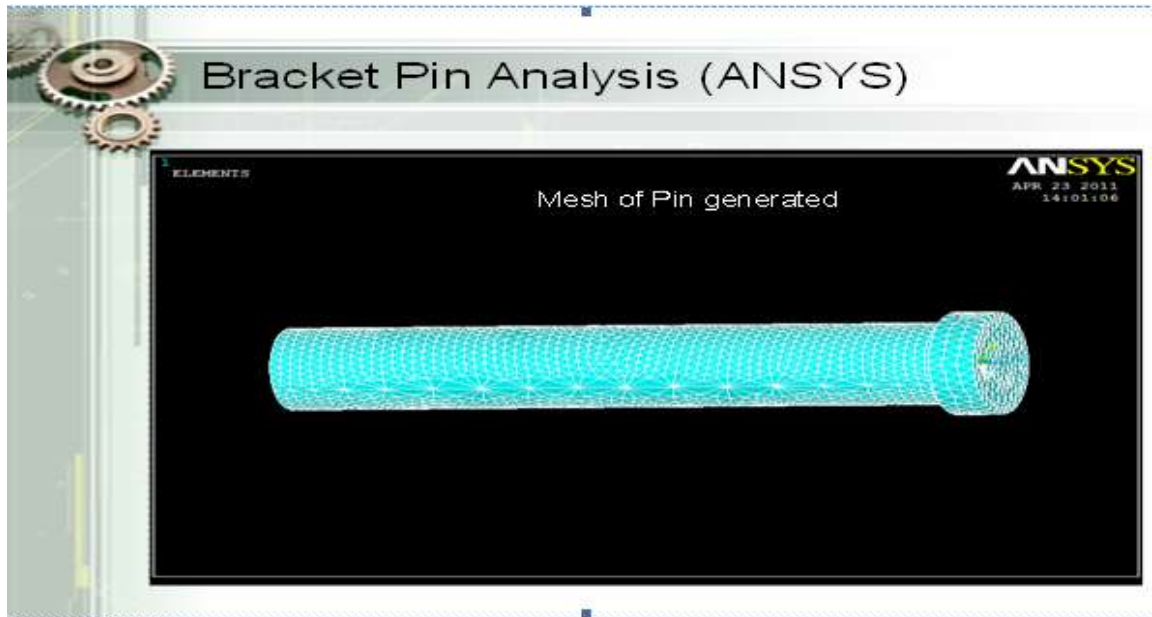


Figure – 5.20 Mesh on Pin with ANSYS

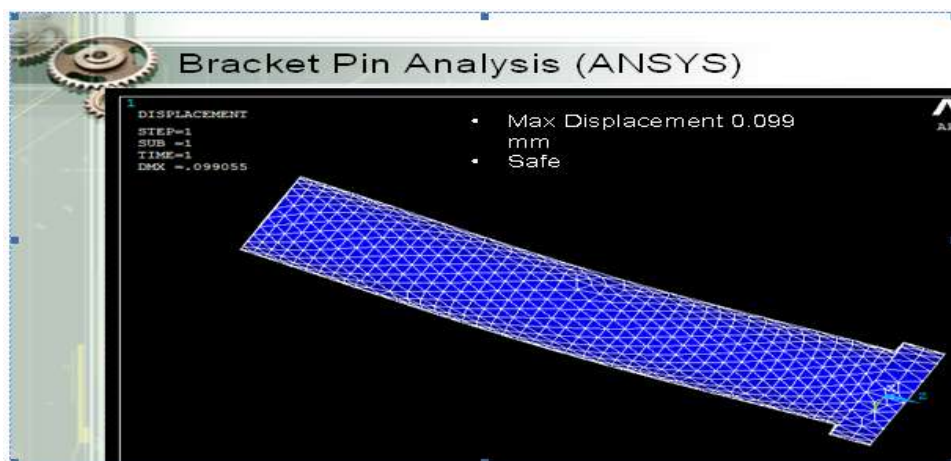
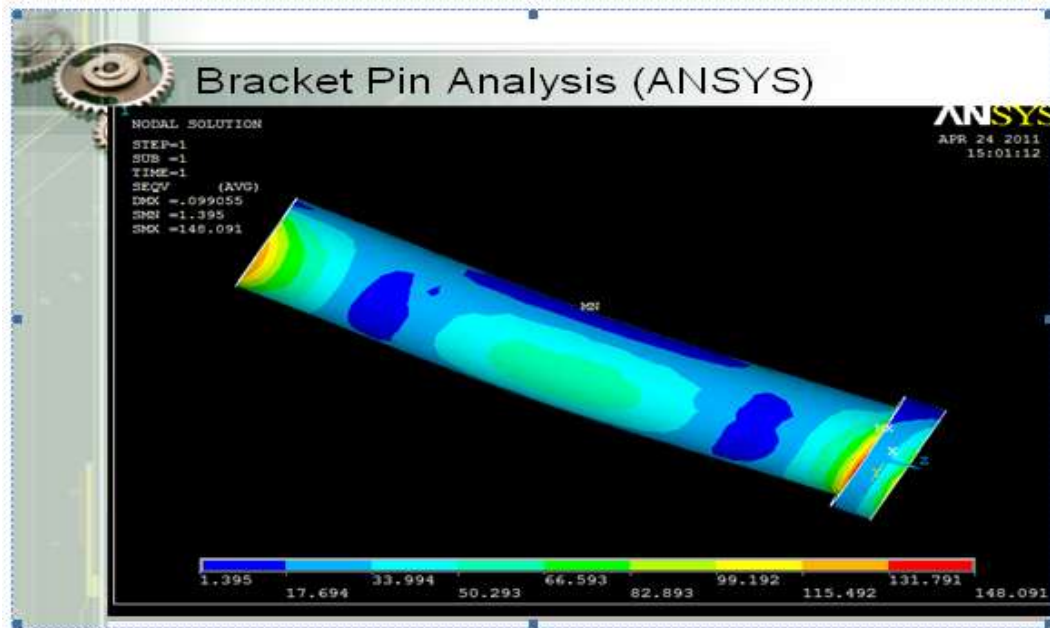


Figure – 5.21 Displacement of Pin



**Figure – 5.22 Von Mises Stress**

#### **5.4.15 BRACKET PIN'S RESPONSE IN STRESS**

It has max Von Mises stress of 148 MPa and displacement of 0.099 mm the pin is safe under the loading conditions.

#### **5.4.16 BRACKET ASSEMBLY'S ANALYSIS IN MECHANICA**

Bracket plate was constrained from the both sides; load on each bracket was distributed by dividing  $F_x$  and  $F_y$  by 4. Coarse mesh was applied.

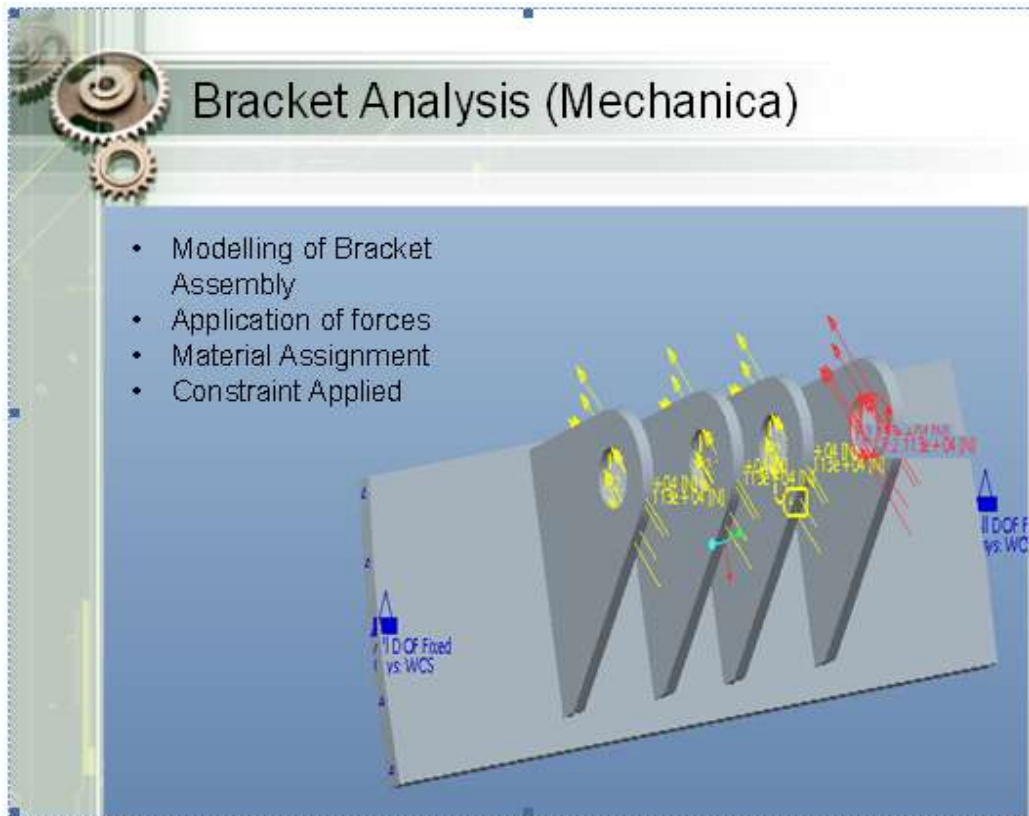


**Figure – 5.23 Forces Applied on Bracket Assembly**

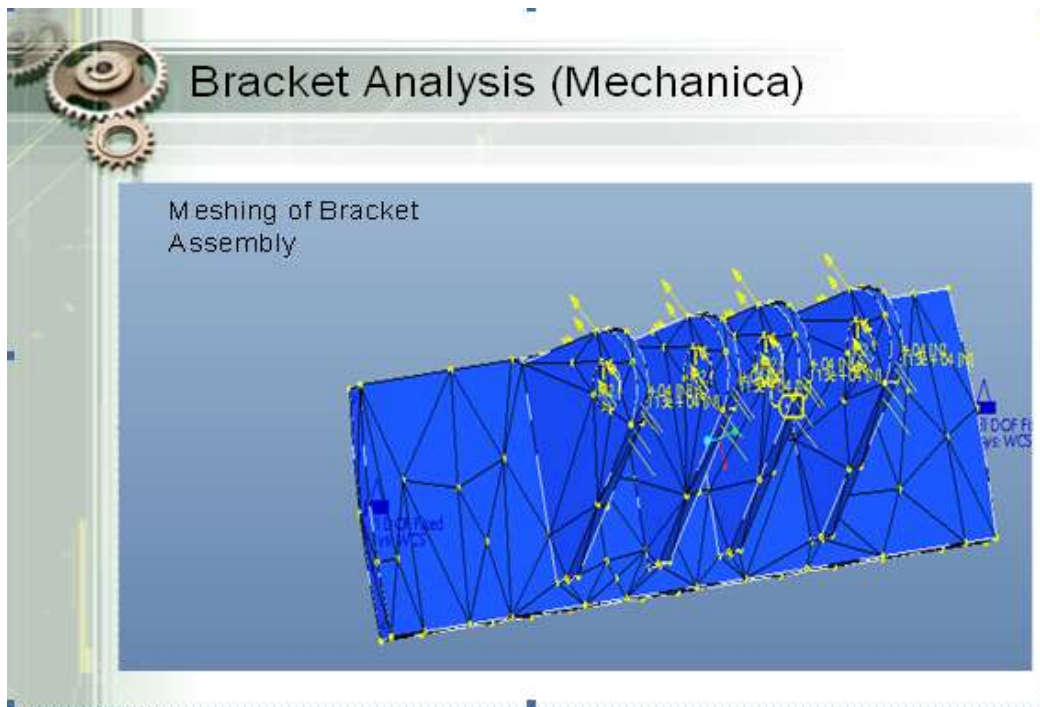


**Figure – 5.24 Meshing of Bracket Assembly**

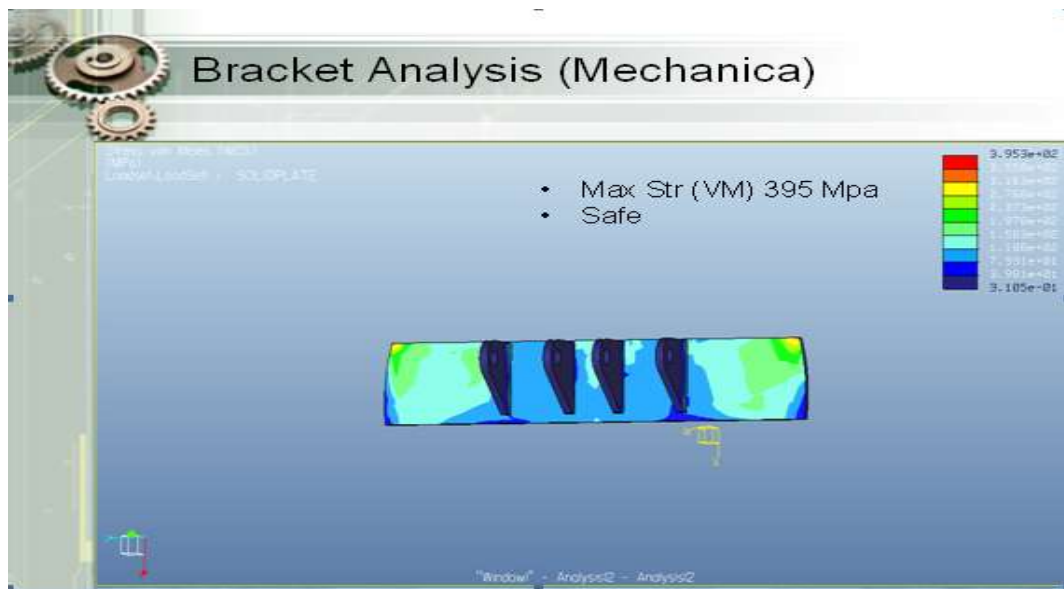


**Figure – 5.25 Von Mises Stress on Bracket Assembly**

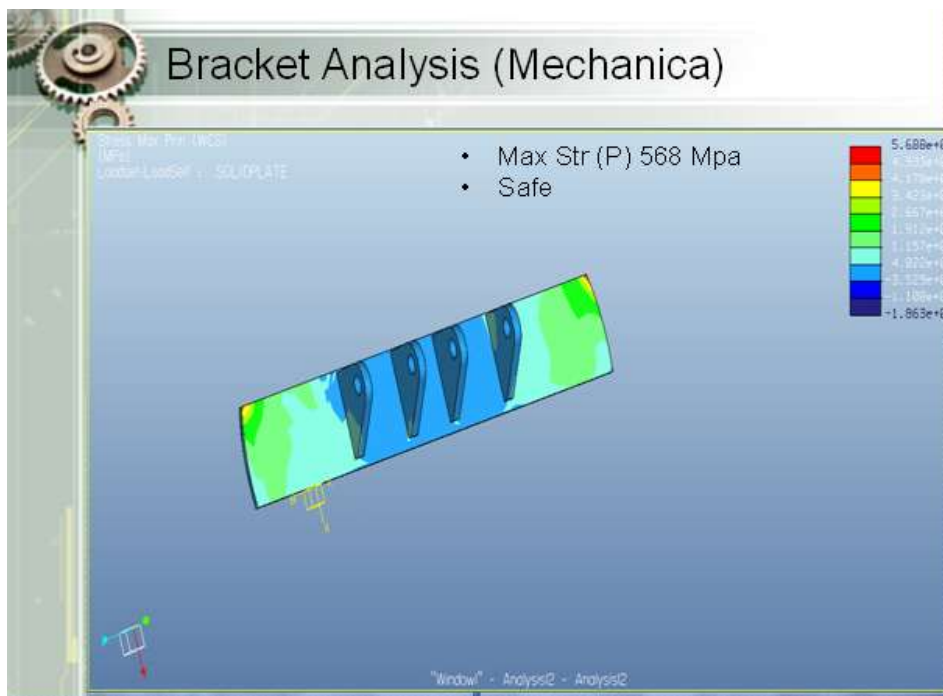


**Figure – 5.26 Max Principal Stress on Bracket Assembly**

#### 5.4.15 BRACKET ASSEMBLY'S RESPONSE IN STRESS (MECHANICA)

It has max Von Mises stress of 395 Mpa, assembly seems failed under the loading conditions, but has shown deflection due to bending moments.

#### 5.4.16 BRACKET ASSEMBLY'S ANALYSIS IN ANSYS

Bracket plate was constrained from the both sides; load on each bracket was

distributed by dividing  $F_x$  and  $F_y$  by 4. Mapped mesh was applied.

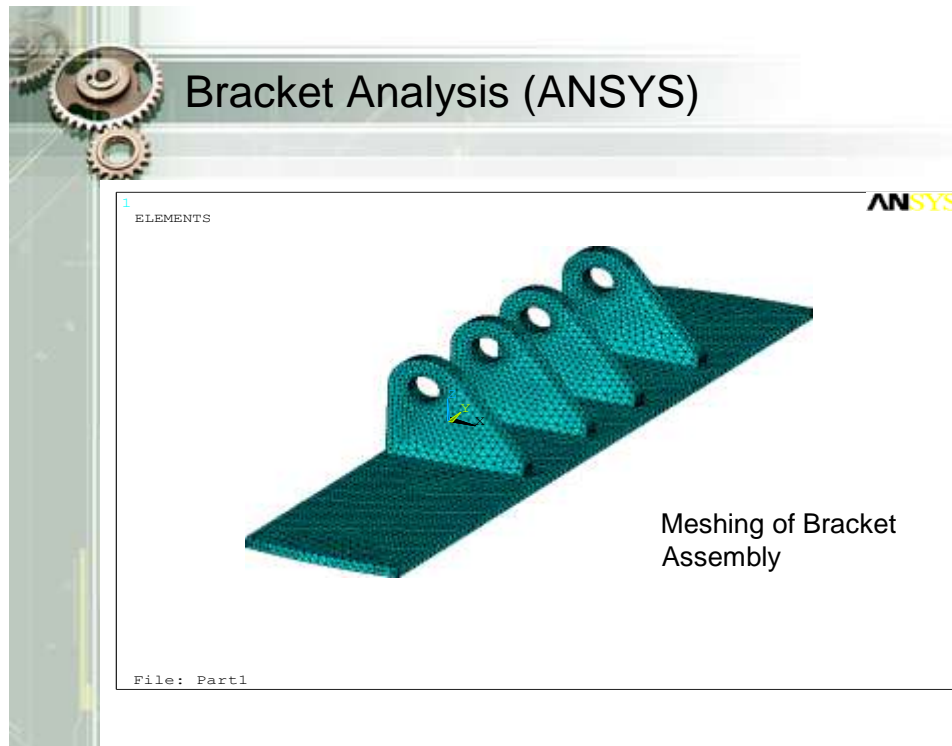


**Figure – 5.27 Meshing of Bracket Assembly**

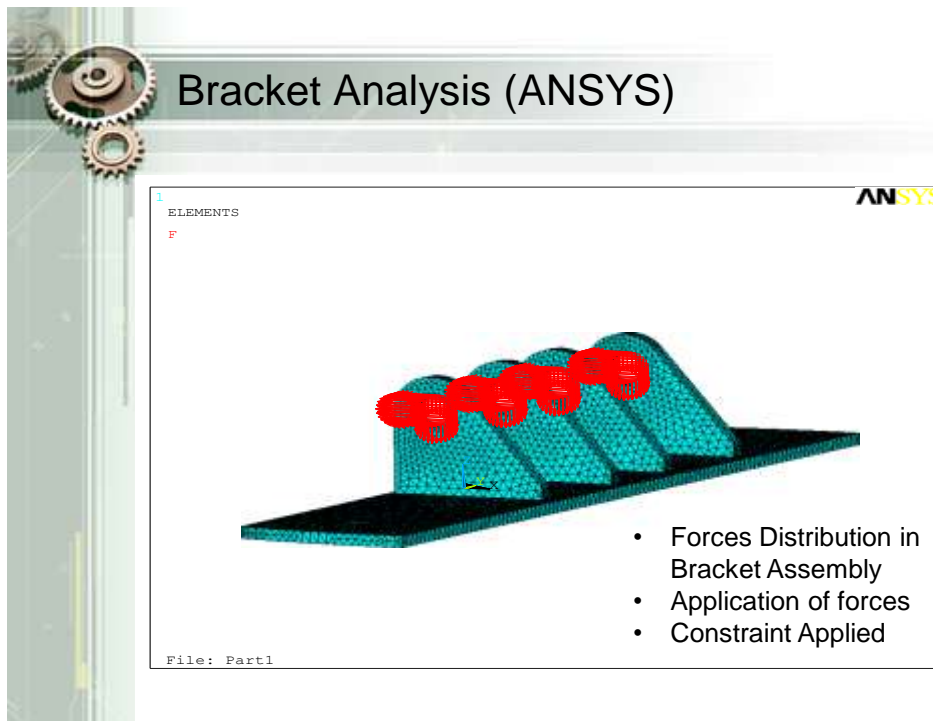


**Figure – 5.27 Forces Applied on Bracket Assembly**

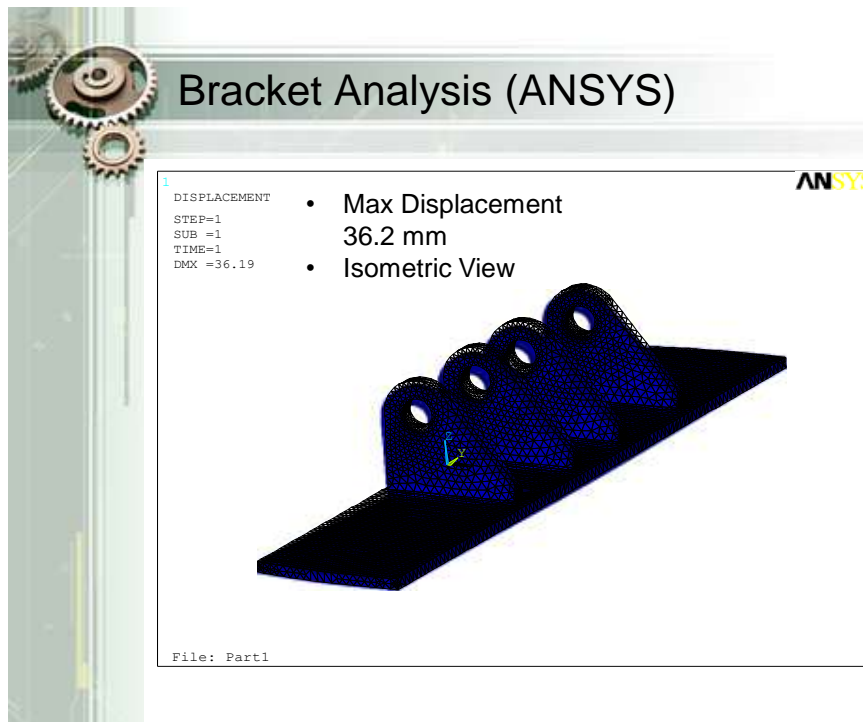


**Figure – 5.28 Failure of Bracket Assembly**

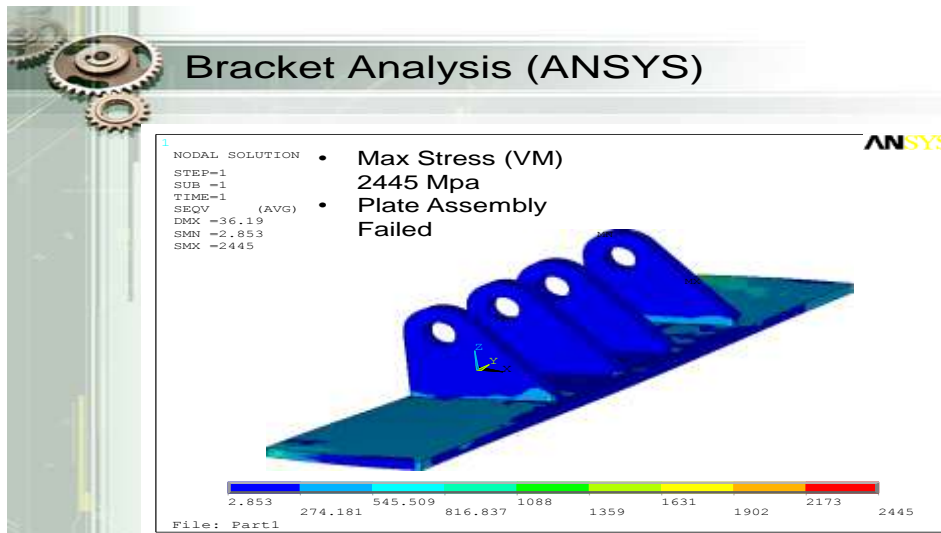


**Figure – 5.29 Von Mises Stress on Bracket Assembly**

#### 5.4.15 BRACKET ASSEMBLY'S RESPONSE IN STRESS (ANSYS)

It has max Von Mises stress of 2445 Mpa, assembly seems failed under the loading conditions, but has shown deflection of 36 mm due to bending moments.

## 5.5 COMPARISON OF RESULTS OF ANSYS AND MECHANICA

Type of Work	ANSYS	Mechanica	Assessment
Modelling	Difficult	Easy	Modelling is easy in Proe Mechanica, so things modelled in Proe can be imported by ANSYS, so Proe makes easier for ANSYS to model components in 3D
Von Mises Stress Analysis	Gives higher values of stress, closer to practical values	Gives lower values of stress, makes any failing system safe	ANSYS is better for Analysis. In case of Bracket assembly results were same.
Displacement Values	Gives higher values closer to practical problems	Gives values lesser than practical problems	ANSYS is better for Analysis
Principal Stress Analysis	Gives higher values of stress, closer to practical values	Gives lower values of stress, makes any failing system safe	ANSYS is better for Analysis
Shear Stress Analysis	Gives higher values of stress, closer to practical values	Gives lower values of stress, makes any failing system safe	ANSYS is better for Analysis

# CHAPTER 6

## 6. RECOMMENDATIONS

- a. Necessary reinforcement be provided to base plate to reduce deflection due to bending moments for improved design and safe handling/operation of bridge equipment
- b. Side swaying can produce moments, to reduce/cater for this tendency reinforcement be provided to top hull brackets to withstand the sideward forces.
- c. Surface treatment / case hardening of bearing surfaces i.e. pins, brackets, etc be carried out to avoid erosion/stress concentration.
- d. Validation of improved designed parts (as stated above) be carried out prior to installation in the hull of MBT

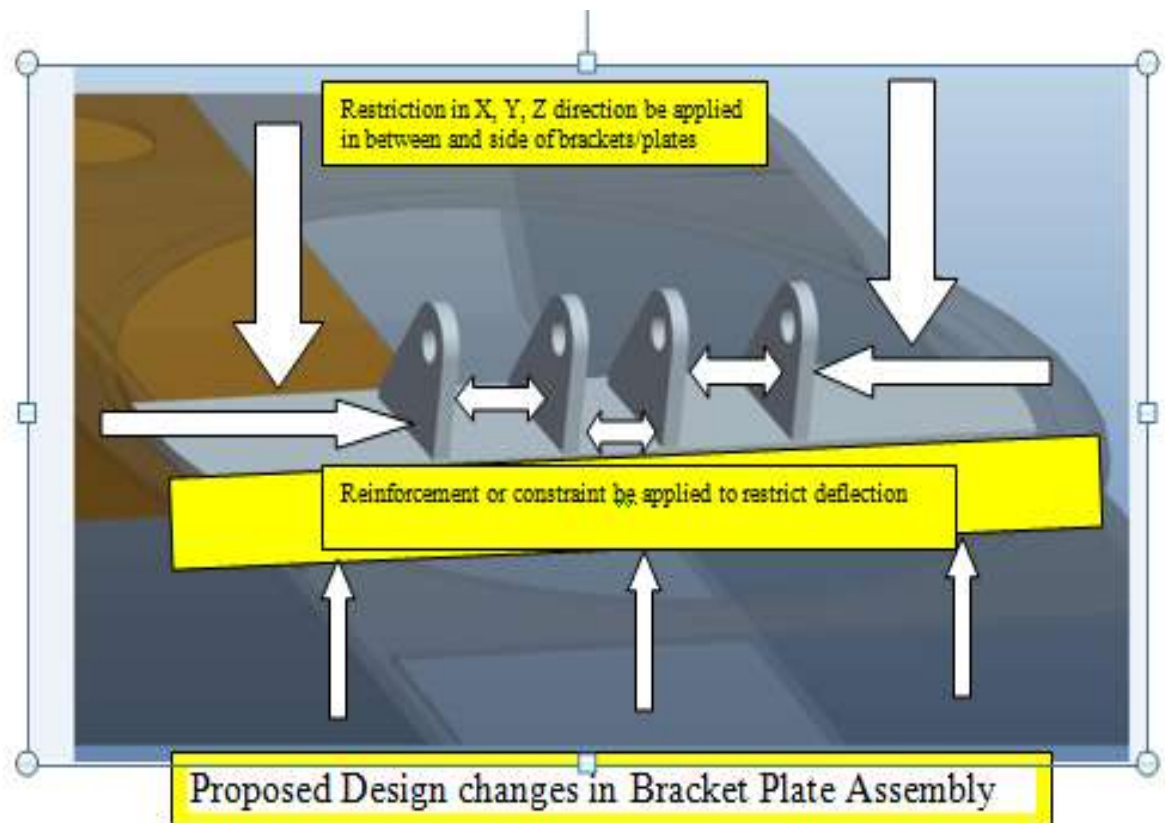
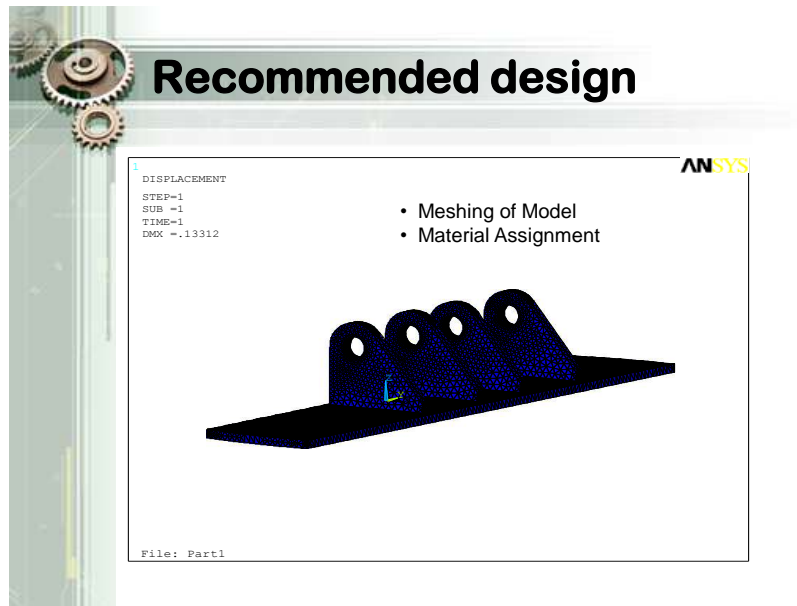


Figure – 6.1 Proposed Design Changes



## 6.1 ANALYSIS OF RECOMMENDED DESIGN

It was tested for an angular load of 90 Tons and proved safe in the static analysis by using ANSYS. However, it is safe for any load of below 70 tons as analysed in static analysis.



**Figure – 6.2 Mesh Applied**

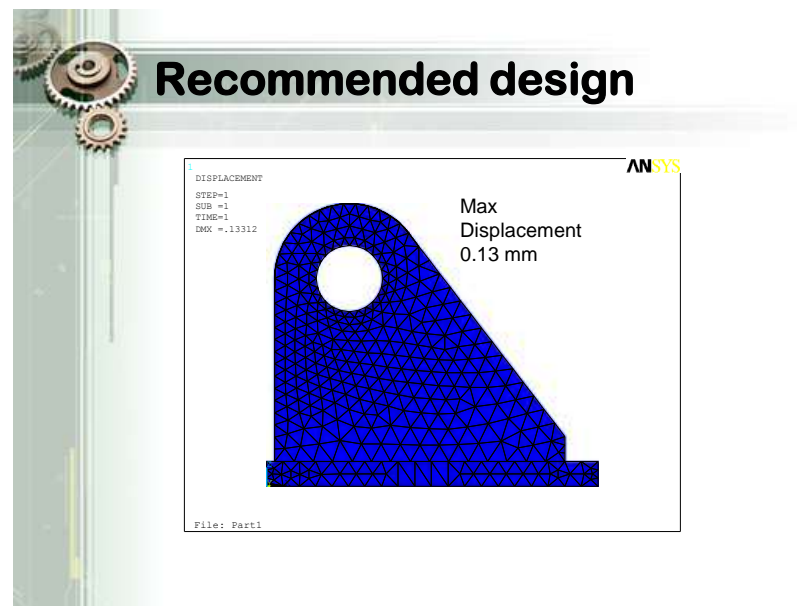


**Figure – 6.3 Displacement**

## 6.2 CONCLUSION

The results achieved from both Proe and ANSYS were almost similar in some cases and different in some parts analysis. For R&D tasks in defence industry; university-manufacturer collaboration is necessary. All impediments of indigenization can be removed by promoting innovative ideas and original work. This will promote greater participation of private sector in meeting core defence requirements. Universities and students can always be handy to assist by implementation and analysis of designs to support the vital cause of national defence.

## REFERENCES

1. Von Mises, R. (1913). *Mechanik der festen Körper im plastisch deformablen Zustand*. Göttingen. Nachr. Math. Phys., vol. 1, pp. 582–592.
2. Ford, *Advanced Mechanics of Materials*, Longmans, London, 1963
3. Hill, R. (1950). *The Mathematical Theory of Plasticity*. Oxford, Clarendon Press
4. S. M. A. Kazimi. (1982). *Solid Mechanics*. Tata McGraw-Hill. ISBN 0074517155, pp. 76-78.
5. Juvinal, Robert C. & Marshek, Kurt .; *Fundamentals of machine component design*. – 2nd ed., 1991, pp. 217, ISBN 0-471-62281-8
6. AMIR R. KHOEI; *Computational Plasticity in Powder Forming Processes*; Elsevier, Amsterdam; 2005; 449 pp.
7. MAO-HONG YU; "Advances in strength theories for materials under complex stress state in the 20th Century"; *Applied Mechanics Reviews*; American Society of Mechanical Engineers, New York, U.S.A.; May 2002; 55 (3): pp. 169–218.
8. NIELS SAABYE OTTOSEN and MATTI RISTINMAA; *The Mechanics of Constitutive Modeling*; Elsevier Science, Amsterdam, The Netherlands; 2005; pp. 165ff.
9. Coulomb, C. A. (1776). *Essai sur une application des regles des maximis et minimis a quelques problemes de statique relatifs, a la architecture*. Mem. Acad. Roy. Div. Sav., vol. 7, pp. 343–387. Slaughter, W. S., 2002, *The Linearized Theory of Elasticity*, Birkhauser.
10. Arnold (1964). *Mechanics of Deformable Bodies*. New York: Academic Press.
11. Landau (1986). *Theory of Elasticity* (3rd ed.). Oxford, England: Butterworth-Heinemann. ISBN 0-7506-2633-X.
12. Bousenque, Josef (1885). *Application des potentiels à l'étude de l'équilibre et du mouvement des solides élastiques*. Paris, France: Gauthier-Villars. <http://name.umd.umich.edu/ABV5032.0001.001>.
13. Mindlin, R. D. (1936). "Force at a point in the interior of a semi-infinite solid". *Physics* 7 (5): 195–202. doi:10.1063/1.1745385.
14. Hertz, Heinrich (1882). "Contact between solid elastic bodies". *Journ. Für reine und angewandte Math.* 92.
15. [en.wikipedia.org/wiki/Dynamic\\_mechanical\\_analysis](http://en.wikipedia.org/wiki/Dynamic_mechanical_analysis) –
16. [en.wikipedia.org/wiki/Euler-Bernoulli\\_beam\\_equation](http://en.wikipedia.org/wiki/Euler-Bernoulli_beam_equation)
17. T. R. Chandupatla, A D Belegundu, *Introduction to Finite Element in Engineering*, PHI-2000, pp 535-536.
18. Charles E Knight, Jr., *The Finite Element Method in Mechanical Design*, PWS-KENT Publishing Company-1997.
19. V. Ramamurti, *Computer Aided Mechanical Design & Analysis*, Tata McGraw Hills-2000, pp 137-139.

20. [Johansson & S, Eslund](#), Optimization of Vehicle Dynamics in Truck by use of Full Vehicle FE Models, [I.Mech.E.](#)- C466/016/93, pp 181-193,1993
21. [H J Beermann](#), English translation by [Guy Tidbury](#), The Analysis of Commercial Vehicle Structures, [Verlag TUV Rheinland GmbH](#) Koln-1989, pp 456-457.
22. John Fenton, Handbook of Automotive Body Systems Design, Professional Engineering Publishing-1998, pp 357.
23. W. D. Collins, Some axially symmetric stress distributions in elastic solids containing penny-shaped cracks.2000, pp 324.
24. [M. Kachanov](#), A simple technique of stress analysis in elastic solids with many cracks. [Int. J. Fracture](#) 28, R11-R19 (1999), pp 98-101.
25. [P. Datsyshin](#) and [M. P. Savruk](#), A system of arbitrarily oriented cracks in elastic solids. / [Appl. Math. Mech. \(PMM\)](#), translation of the Soviet journal [Prikl. Mat. Mekh.](#)) 37(2), pp326-332 (1993).
26. [Shigley, J.E.](#), [Mischke, C.R.](#), “Mechanical Engineering Design,” Sixth Edition, McGraw Hill, Boston, 2001, pp 208.
27. [www.wikipedia.org/wiki/inner\\_prod](http://www.wikipedia.org/wiki/inner_prod) referred on 11 April 2010.
28. [www.wikipedia.org/wiki/continuum\\_mech](http://www.wikipedia.org/wiki/continuum_mech) referred on 25 June 2010.
- \*6. R &D centre, Technical report number 13557, Roberto P. Garcia Stephen G. Lambrecht U.S. Army Tank-Automotive Command ATTN: AMSTA-RYC, Finite Element Analysis of The Armored Vehicle Launched Bridge (AVLB) MARCH 1992, pp 23-25.
- \*7 [www.wikipedia.org/wiki/lp\\_space](http://www.wikipedia.org/wiki/lp_space) referred on 10 March 2010.